1 Introduction

In nature, high quality potable water results from rain (or snow). Most rain results from the solar evaporation of sea water, followed by condensation in the atmosphere. That is, from a natural process of distillation.

In the laboratory, water of high purity can likewise be produced by distillation. As the energy required to evaporate water is very high, this process – called simple distillation - is not energy efficient, and not economical for producing large quantities of water. The enthalpy of evaporation of water - about 2.45×10^6 J/kg at 20°C – exceeds the theoretical minimum work required for separating a kilogram of pure water from sea water by a factor of about 800 [16].

But distillation entails both evaporation and condensation. On condensing vapour, about 99.88% of the heat of evaporation of the sea water is recovered – but normally at a lower temperature than the heat supplied for evaporation. Indeed, the higher the temperature difference, the higher the rate of heat transfer, and the higher the production rate from the distiller. In a vapour compression distiller (VCD) the vapour resulting from the evaporation of saline water is compressed, whereby its temperature is raised. What is important is that at the higher pressure, the vapour will condense at a temperature above the evaporation of saline water.

Thus if the evaporation of saline water takes place on the outside of a set of heat transfer tubes, then condensation of the vapour into pure water takes place inside this same set of tubes, after the vapour has been compressed. The very large latent heat of evaporation/condensation is efficiently recycled, by which the total energy requirement is drastically reduced. Indeed, in a well designed well-insulated VC distiller with a suitable counterflow heat exchanger for heat recovery, the primary energy input during steady operation is to the vapour compressor (and much smaller amounts to the water circulation pumps and vacuum pump). Except during start-up, no heat input is needed during operation.

The main energy needed is to compress the vapour and raise its pressure - and thereby

raise its saturation (condensing) temperature sufficiently above the evaporation temperature for effective heat transfer from the condensation inside the tubes through the heat exchange tube walls to the evaporation of saline water outside them.

This chapter provides some background by describing the need for widespread use of inexpensive and reliable desalination technologies, and defines the thesis objectives. Some attention is also given to the most used distillation technologies, especially vapour compression distillation.

1.1 Background

All terrestrial species, including humans, depend heavily on fresh water. Humans use water for different basic purposes, such as drinking, cooking, washing and sanitation. Human development and civilization requires a reliable supply of fresh water. However, the amount of *non-saline* water available on earth is less than 3% of the water on earth [1] - much of it locked up in glaciers and ice sheets.

As living standards develop, water consumption increases. The demand for potable water is increasing however, not only because of rising domestic and urban consumption but also to meet the needs of industry & agriculture. The improvement of living conditions is slow or is not happening in many "developing" countries. In these countries a considerable number of people still lack clean drinking water and have to use contaminated water. According to the World Health Organization, contaminated drinking water is involved in 80% of all human illnesses and diseases (gastroenteritis, dysentery, cholera, and other waterborne diseases) which claim many lives each year.

Fresh water is an essential commodity both for developed and developing countries. The biggest challenge many countries are facing is to ensure that enough water resources are available for future generations. This will require from some countries, especially in water-scarce regions, a reduction of water wastage and a better water conservation strategy.

The demand for potable water due to the rapid increase of world population, the rising domestic consumption, and increasing needs of the industry and irrigation, cannot be fully

satisfied by the natural sources of water supply (e.g. rain, rivers). Therefore other means of water production have to be found to supplement these natural sources. Several attempts have been made to solve this problem through better water conservation and demand management or by building more, costly dams. The increasing population and increasing *per capita* consumption cannot in the long run be satisfied by these measures alone.

An alternative way to supplement water for human consumption is the artificial desalination of seawater. Due to technological improvements, desalinated seawater is becoming more and more viable as an alternative water source for many applications, and in many regions.

Thus by the end of 2001, a total of 15, 233 large desalinating plants (each over 100 m^3 per plant) had been installed or contracted over the previous decades, with a total capacity of 32.4 million cubic metres per day [4]. This represents a *doubling in world desalination capacity* - **in less than 24 months!** In the same 2 years, the *seawater desalination capacity grew by 140%!*

Saudi Arabia (18.7%), the USA (15.8%) and the United Arab Emirates (14.6%), had the biggest share of the total desalination capacity [4].

Desalination of seawater is at present the major source of potable water in arid coastal regions such as the Arabian Gulf region. Most of the countries there rely to a large extent on desalination in order to supply their increasing fresh water requirement.

1.2 Thesis Objectives

This thesis describes research in the field of desalination for the production of potable water: Vapour compression distillation (VCD) using thin high density polyethylene (HDPE) and polypropylene (PP) film heat transfer elements in a laboratory model. The aim is to design, build and test this model desalinator.

The model is to enable us to:

- ✦ understand and improve the energy efficiency of a desalinator by using air mattress-

like polymer heat transfer elements instead of metal heat transfer tubes.

- develop methods to further increase the energy efficiency of the model.

The activities carried out for the accomplishment of the specific objectives are listed in chapter 2.

1.3 Desalination Technologies

Over the past century several processes have been developed for desalination, including evaporative processes (distillation), reverse osmosis, electrodialysis, freezing, and other crystallization processes. Some of these processes are of no economical importance. At present, developments concentrate on three general processes, namely, membrane processes, crystallization and distillation.

In the membrane processes, (reverse osmosis and electrodialysis), desalination occurs without phase change.

In reverse osmosis, saline water is forced under high pressure through a semi-permeable membrane which allows mainly fresh water to penetrate. It was originally applied to desalination of brackish water but successive developments have shown its viability for desalination of seawater.

Electrodialysis uses an electric field placed across the membranes to move salt ions out of the solution via the membranes. It is mainly applied for desalination of water sources with low salinity (due to energy required with increasing salt content) sometimes in the presence of hydrocarbons or clathrates.

Crystallization is characterized by phase change from liquid to solid. The obtained ice crystals contain pure water. However, brine clings to the surface of the ice crystals, and the needed washing with pure water makes the process inefficient.

Distillation is the oldest method of desalination. It was employed for the first time over 400 years ago [7] for production of fresh water from seawater. Modern distillation includes three processes: multi-effect distillation (MED), multistage flash distillation

(MSF), and vapour compression distillation (VCD).

All traditional desalination systems do have some constraints: high energy consumption, high initial cost, corrosion and scaling of the heat transfer surfaces. In the following sections the three distillation processes are described.

1.3.1 Multi-Effect Distillation

Multi-effect distillation (MED) was developed around 1900 in replacement of the existing simple stills (single effect) used over centuries. The single effect stills were *bulky* and *inefficient* due to factors such as high energy consumption due to the high heat of evaporation of water, severe scaling, and the carry-over of saline droplets into the distillate. The introduction of the multi-effect (MSF) process reduced scaling - which can be very efficiently managed in this process today [14,15]. Later the change from pool boiling to film boiling (in MED and VCD) enabled a much lower ΔT and a more or less proportional decrease in primary energy consumption.

Distillation involves evaporation of saline water, followed by condensation of the vapour, in which nearly all of the heat of evaporation can be recovered – at a lower temperature. In a simple (single effect) still, the heat of condensation is rejected to the environment by a cooling system.

In a multi-effect system, however, the heat of condensation is used to evaporate more saline water at a lower temperature. Figure 1.1 illustrates, in a schematic way, the principle of MED. Steam at 60°C in the leftmost chamber flows (arrows), condenses (dotted line) on a thin heat transfer surface (single solid line) and gives up heat of condensation, which passes through the surface to its cooler side. Saline water (dashed) trickling down as a film on this cooler side of the surface receives the heat, and is partly evaporated to form more vapour at say 58°C. This vapour flows (arrows) and condenses (dotted) on the next heat transfer surface, causing more (dashed) saline water to evaporate on its opposite side. Condensed vapour (dotted) collects as pure water (distillate – honeycomb) on the left of the heat transfer surfaces, and concentrate brine (dashed) on theright. In this simplified diagram, each chamber represents an "effect". The multi-effect distillation technology has been applied in industry for some decades - for example,

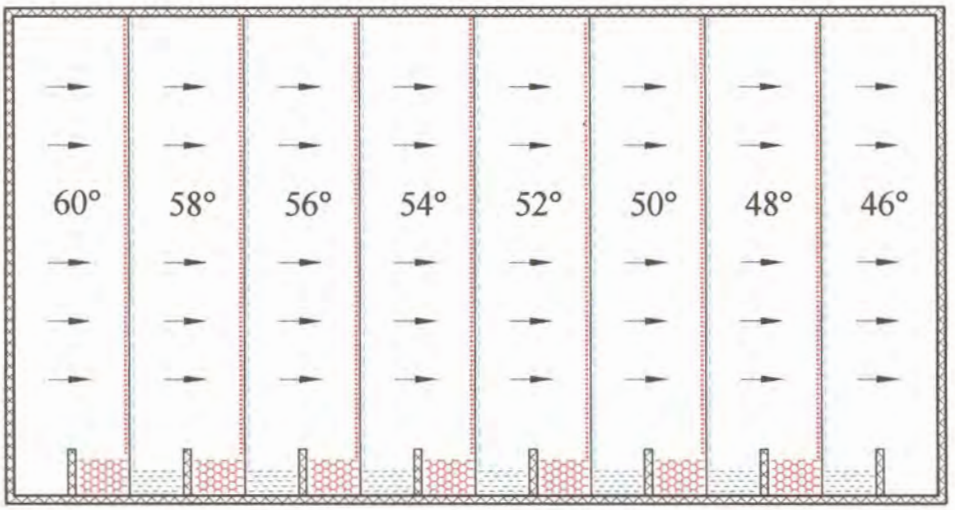

Fig. 1.1 Principle of multi-effect distillation.

in sugar production. Although thermodynamically more efficient than the Multistage Flash (MSF) process, the MED share of total desalination decreased from 1960 to 1998. The reason for its displacement by the simpler MSF process is its relative complexity, and problems with scaling and fouling at high temperatures.

Modern MED systems operate at lower temperature (LTMED) which has contributed to the renewed interest in this process. The operation at low temperature greatly reduces the scaling potential as saline water is kept below the saturation condition for low solubility salts. This also allows the employment of less expensive materials which reduces the capital cost and consequently the water cost.

1.3.2 Multistage Flash Distillation

Multistage flash distillation (MSF) for seawater desalination was proposed in the early 1950's by Prof. R.S. Silver as an alternative to overcome scaling problems affecting the heat transfer surfaces of MED units. As result of its "*morphological simplicity*" [6] MSF soon became the dominant desalination process for production of fresh water from seawater. 43.5% of world's seawater desalination is by multi-stage flash distillation [4].

Figure 1.2 shows the conceptual design of a MSF process. MSF technology uses steam as its primary energy source. The saline water is pumped through all stages in succession, where it is preheated by vapour condensing on outer tube surface. The condensation of external steam in the brine heater further heats this preheated water to just below its

boiling point. It then enters the first evaporation chamber (stage) at reduced pressure. This, results in flash boiling of part of the raw water.

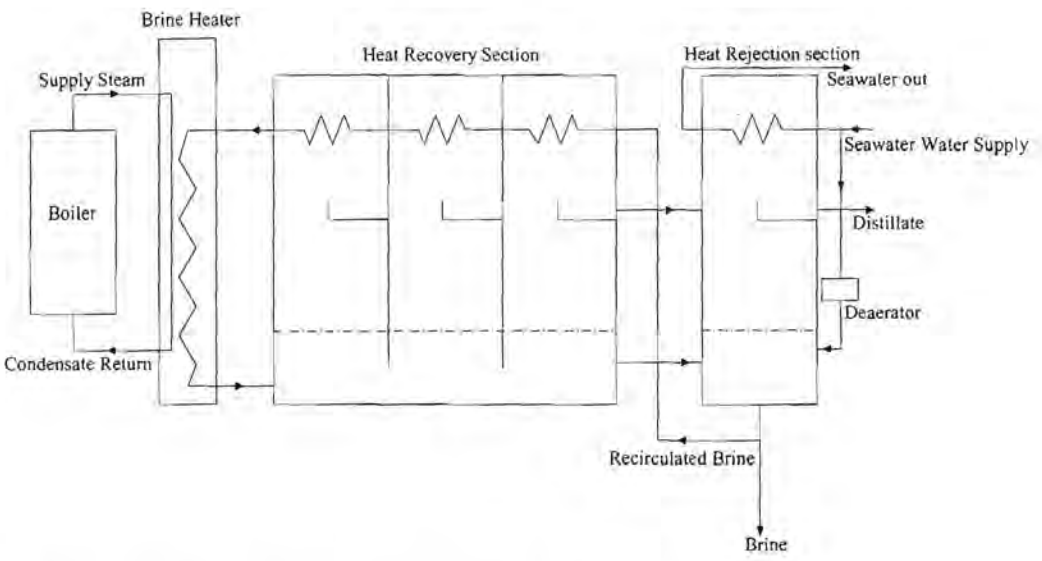

Fig. 1.2 Simplified flow diagram of multistage flash distillation.

Consequently, vapour is released in quantity in striving for equilibrium with conditions of the stage. It then condenses on the outer surface of the stage tubes. Both the condensate and the unevaporated brine flow into the next stage. More vapour is produced from the brine due to the drop in pressure in the stage. The process repeats itself in the remaining stages resulting in the production of more distillate. The condensate produced in all stages is collected and the concentrated brine is discharged before being used in the pre-heating of further incoming raw water.

The energy efficiency (G O R or performance ratio R) of a MSF plant depends on the *ratio* of the overall temperature range ΔT_{ov} to the typical (log mean) temperature difference ΔT_{l} between the flashing brine and the saline water being heated in the tubes [10]. If the number of stages is too small, this will negatively affect either R or the productivity of the still.

1.3.3 Vapor Compression Distillation

1.3.3.1 Historical Perspective

Vapour compression distillation (VCD) technology was developed by the military during

World War II to improve fuel efficiency. It is the most thermodynamically energy efficient single-purpose distillation process. It takes two forms: thermal (TVC) and mechanical (MVC). The former process uses a supersonic jet from high-pressure steam to drive an ejector (thermocompressor) to compress vapour to a required pressure. The latter compresses vapour using mechanical energy from an electric motor or a diesel engine.

Both configurations operate at low temperature difference between the boiling and the condensing water, thus minimizing the system's energy consumption.

The first VC units employed diesel engines to drive the compressor and operated slightly above atmospheric pressure. Though these units met the urgent need of the military a great deal of maintenance (scale removal, and maintenance of the diesel engines) was required to maintain the desired performance. Diesel units were replaced by electrically driven ones because of their short life under continuous operation conditions. In this way the maintenance needs were reduced, but scale was still affecting the operation of the systems. This problem was overcome with the development of units operating under vacuum. Hence, the operation at lower temperature was possible as it is in most modern vapour compression and multi-effect systems.

Mechanical vapour compression is especially for applications where heat/steam is not readily available, and has so far been used in relatively small units - up to about 1,500 m^3 per day [17].

The mechanical vapour compression (MVC) process is dealt with in more detail in the next section.

1.3.3.2 Basic Functioning Principle of MVC

The basic principle of mechanical vapour compression (MVC) technology is depicted in figure 1.3. Vapour from heated saline water flowing in a thin film on a tube's surface, is compressed by a compressor to a saturation temperature that is 2 to 3°C above the evaporation temperature. This is done to offset the boiling point elevation on the evaporating side and to provide the required small temperature difference for the heat

transfer process [7].

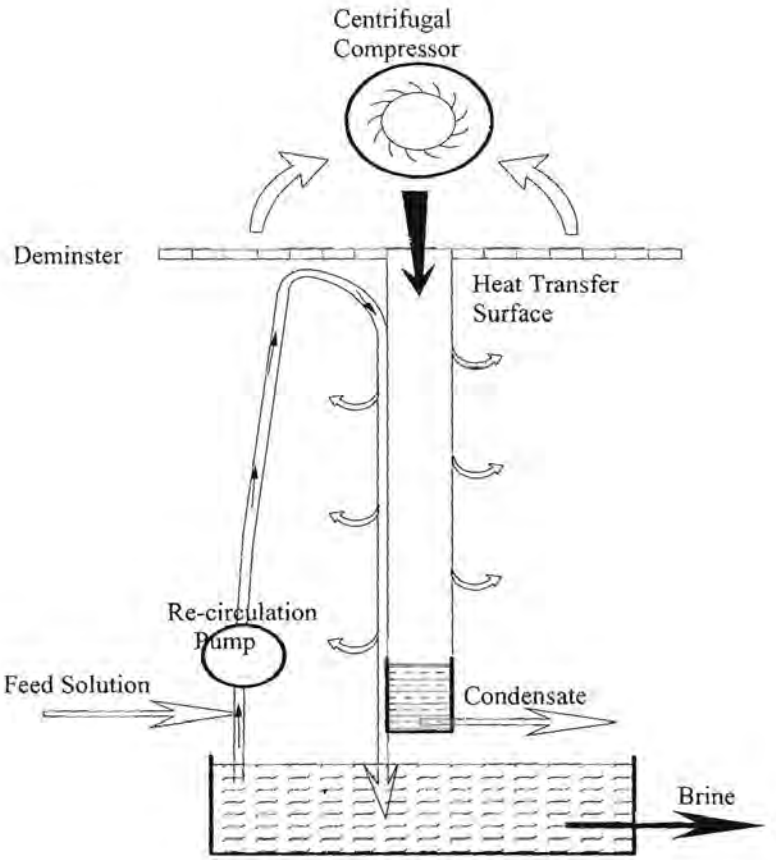

Fig.1.3 Basic principle of vapour compression

The compressed vapour is introduced on the other side of the tubes, where it condenses. The heat of condensation is conducted through the tube wall to the evaporating side, where it provides the heat of evaporation for saline water. The condensate flows downwards and is discharged as distillate. The brine (concentrated saline water) is partly discharged for disposal and the balance mixed with the feed solution. The mixture is pumped again onto the tube surface for further evaporation.

1.3.3.3 Temperature - Entropy Chart

An approximation of the vapour compression process can be represented on the temperature-entropy diagram, depicted in figure 1.4. According to the diagram, evaporation of portion of the feed occurs at constant temperature represented by the line $1' \rightarrowtail 1$.

The obtained vapour is compressed from state point 1 to 2 before condensing along the isobar $2 \rightarrowtail 3$. As a result, distillate is produced along the horizontal line which ends at

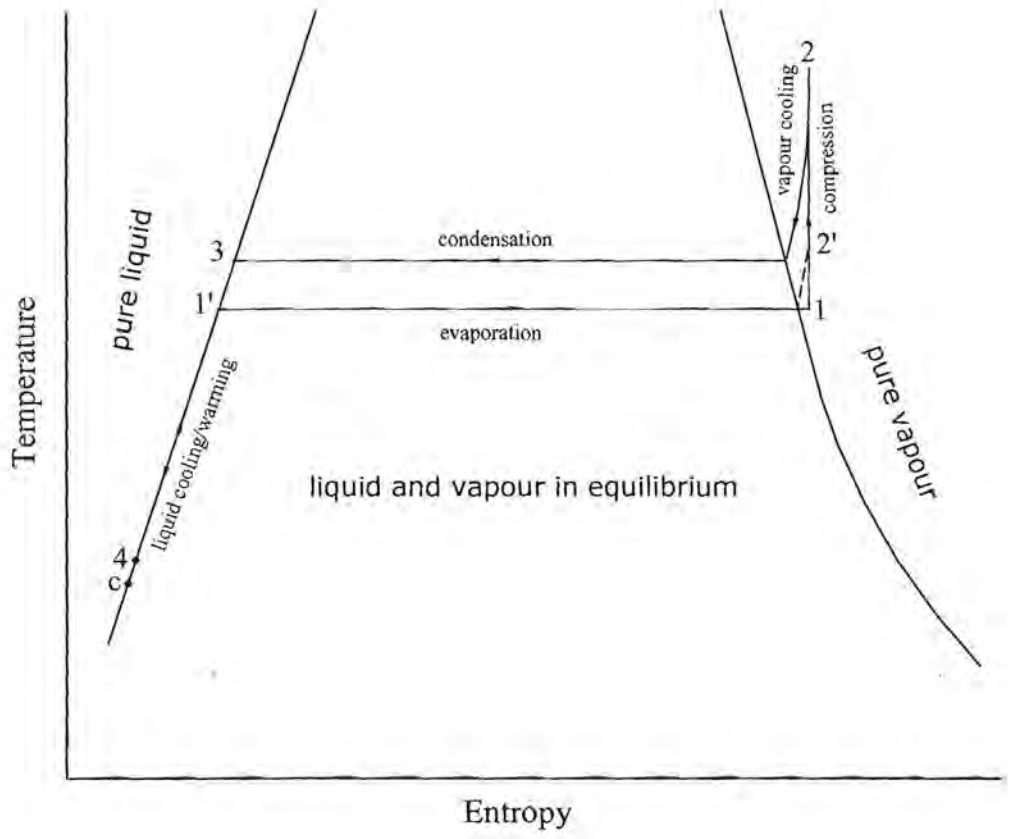

Fig. 1.4 Temperature - entropy chart of vapour compression process [7].

state point 3. The distillate is cooled by passing through a liquid-liquid heat exchanger and discharged at 4. The brine (non-evaporated portion of the feed) passes also through the heat exchanger, thus being cooled in the process, from 1' to 4, and discharged at this temperature. The feed solution enters the heat exchanger at a temperature t_c below that at 4 and is heated to a temperature slightly less than at 1'. The additional temperature required for evaporation (at 1') is provided by the condensation of compressed vapour from the compressor.

The processes are described below using equations and the following is assumed:

(a) the temperature of the feed solution at the evaporator is exactly at 1', instead of being

slightly less than that at 1',

(b) the compression is isentropic,

Then the heat balance on the evaporator is

$$\dot{m}(h_2 - h_3) = \dot{m}(h_1 - h_1') \tag{1.1}$$

where $\dot{m}$ is the production rate and h the specific enthalpy (enthalpy per unit mass).

On the liquid-liquid heat exchanger the heat balance is given by

$$\dot{m}_f c(t_1 - t_c) = \dot{m}c(t_3 - t_4) + \dot{m}(\frac{\dot{m}f}{\dot{m}} - 1)c(t_1 - t_4) \tag{1.2}$$

where $\dot{m}_f$ is the feed supply rate, t the temperature, and c the specific heat. The heat transfer in the evaporator is given by

$$\dot{m}(h_2 - h_3) = UA\Delta t_m = UA(t_3 - t_1) \tag{1.3}$$

where U is the overall heat transfer coefficient, A the area, and Δt_m the mean temperature difference for heat transfer.

The heat transfer in the heat exchanger is

$$\dot{m}_f c(t_1 - t_c) = U_1 A' \Delta t_m' \tag{1.4}$$

Solving the equation (1.2) and assuming that the specific heats are equal, thus

$$t_4 = t_c + (\frac{\dot{m}}{\dot{m}_f})(t_3 - t_1) \tag{1.5}$$

and from the equation (1.3)

$$t_4 = t_c + (\frac{h_2 - h_1}{c}) \tag{1.6}$$

Comparing both equations the relationships

$$c(t_3 - t_1) = h_2 - h_1 \tag{1.7}$$

is obtained. This result certifies that the energy input must equal the sensible heat involved in changing the temperature of water from that of evaporation to that of condensation.

1.4 Implementation of Results

The output of the research will be valuable for the efficient production of fresh water from seawater or brackish water needed in remote communities which experience problems with drinking water supply, such as the Northern Cape, Limpopo, Botswana, Namibia and Mozambique. The improved technology may also be applied in the process of concentrating industrial effluents.

1.5 Summary

Human development and civilization in general require the availability of fresh water at an affordable price. Traditional water supply sources cannot alone satisfy the increasing demand for potable water.

Desalination can supplement the need for fresh water. As a result of wide experience accumulated over many years different desalination processes were developed. Some of the processes are undergoing major improvements required for efficient large scale production of potable water competitively compared with that obtained from the traditional sources. The improvement of the existing designs and the use of better and inexpensive materials can contribute to the reduction of the cost of desalted water which is obstructing the widespread use of desalination. This is where this thesis makes a contribution.

1.6 References

1. M.K. Darwish and Al Gobaisi, *Sustainable Augmentation of Fresh Water Resources through Appropriate Energy and Desalination Technologies*, Proceedings of IDA conference, Madrid, Spain, 1997.

2. H.G. Heitman, *Saline Water Processing: Desaliantion and Treatment of Seawater, Brackish Water, and Industrial Waste Water*, VCH, Weinheim, 1990.

3. Abu Qdyas H. A., *Environmental Impacts of Desalination Plants on the Arabian Gulf"*, Proceedings of IDA conference, Manama, Bahrain, 2002.

4. R Wiseman, *IDA Desalination Inventory: Installed Capacity Doubles in less than two years*, Desalination & Water Re-use 12/3 (2002), p10 – 13, based on the report 17 compiled by K. Wangnick.

5. K. S. Spiegler, *Salt-water Purification*, Plenum Press, New York, 1977.

6. R. S. Silver, *Seawater Desalination*, In: Desalination Technology Ed A Porteous Applied Science Publishers.

7. E. D. Howe, *Fundamentals of Water Desalination*, Marcel Dekker, New York, 1974.

8. A. F. Mills, *Heat and Mass Transfer*, Irwin, Chicago, 1995.

9. C. F. Schutte, *Desalination – a South African Perspective*, Water Research Commission, 1983.

10. A. Porteous, *Saline Water Distillation Process*, Longman, Norfolk, 1975.

11. Hadwaco Brochure, *A Quantum Leap toward Effluent-Free Industrial Plants*.

12. K. S. Spiegler, *Principles of Desalination*, Academic Press, New York, 1980.

13. J. R. Howarth, *Vapour Compression,* In: Desalinaton Technology, A. Porteous, Applied Science Publishers LTD, 1983.

14. H. Glade, *The Carbonate System in MSF Distillers*, Proceedings of IDA conference, Manama, Bahrain, 2002.

15. E. Ghiazza and A. M. Ferro, *The Scaling of Tubes in MSF Evaporators: A Critical Review across 20 Years of Operation Experience,* Proceedings of IDA conference, Manama, Bahrain, 2002.

16. D.I. Dykstra, *Sea Water Desalination by Falling Film Process*, In: Desalination and Ocean Technology, S.N. Levine, Dover publications INC., New York.

17. N. M. Wade, Technical and Economic Evaluation of Distillation and Reverse Osmosis Desalination Process, Desalination 93(1993) 343 - 3633.

List of Symbols

A : heat transfer surface area (m^2)

c : specific heat (J/kgK)

h : enthalpy (J/m)

$\dot{m}$: production rate (kg/s)

$\dot{m}_f$: feed supply rate (kg/s)

t : temperature (C)

U : overall heat transfer coefficient (W/m^2K)

Δt_m : mean temperature difference for heat transfer (K)

2 Reducing the Cost of Desalinated Water: Polymer Film Heat Transfer Elements

2.1 Introduction

In the last decade the use of desalination to provide potable water – competitive in many situations with that supplied by conventional means – has witnessed an astonishing growth. Thus the world capacity increased more than 100% in the 24 months from 1 January 2000 to 31 December 2001 [1]. Over a longer term, the growth of the desalination industry (at about 12% per annum) is still far above the growth in the world economy (about 2.3%) [11].

Distillation technologies (MSF, MED and VCD) have been improved significantly for durability and availability [2, 3, 4, 6]. These technical improvements, as well as new modes of delivering systems (BOO and BOOT – build, own, operate and transfer) have significantly reduced the cost of desalinated water.

To lower the cost of desalination systems, desalination activities in progress in the last years have focussed on system optimization, larger unit sizes, improved construction methods, and use of more suitable materials. The basic processes and the heat transfer mechanisms have remained unaltered.

The total cost of desalinated water are the *capital* and *operational* costs. The capital cost (per m^3 of distillate) depends on the total capital cost/unit capacity and the system life-time. The latter is confidently predicted [2, 6] to be about 40 years for currently installed state-of-the-art systems with shells of solid duplex stainless steel. The operating cost comprises energy, maintenance and parts, consumables (mainly antiscalant chemicals), and labour. *The major costs are the capital and the energy costs.* Of the capital, the major parts are 40% for the heat transfer surface and another 40% for the shell [7]. Reference [6] gives 25-35% for the heat transfer surface.

Figure 2.1 shows the qualitative relationship between the installed *thermal conductance*

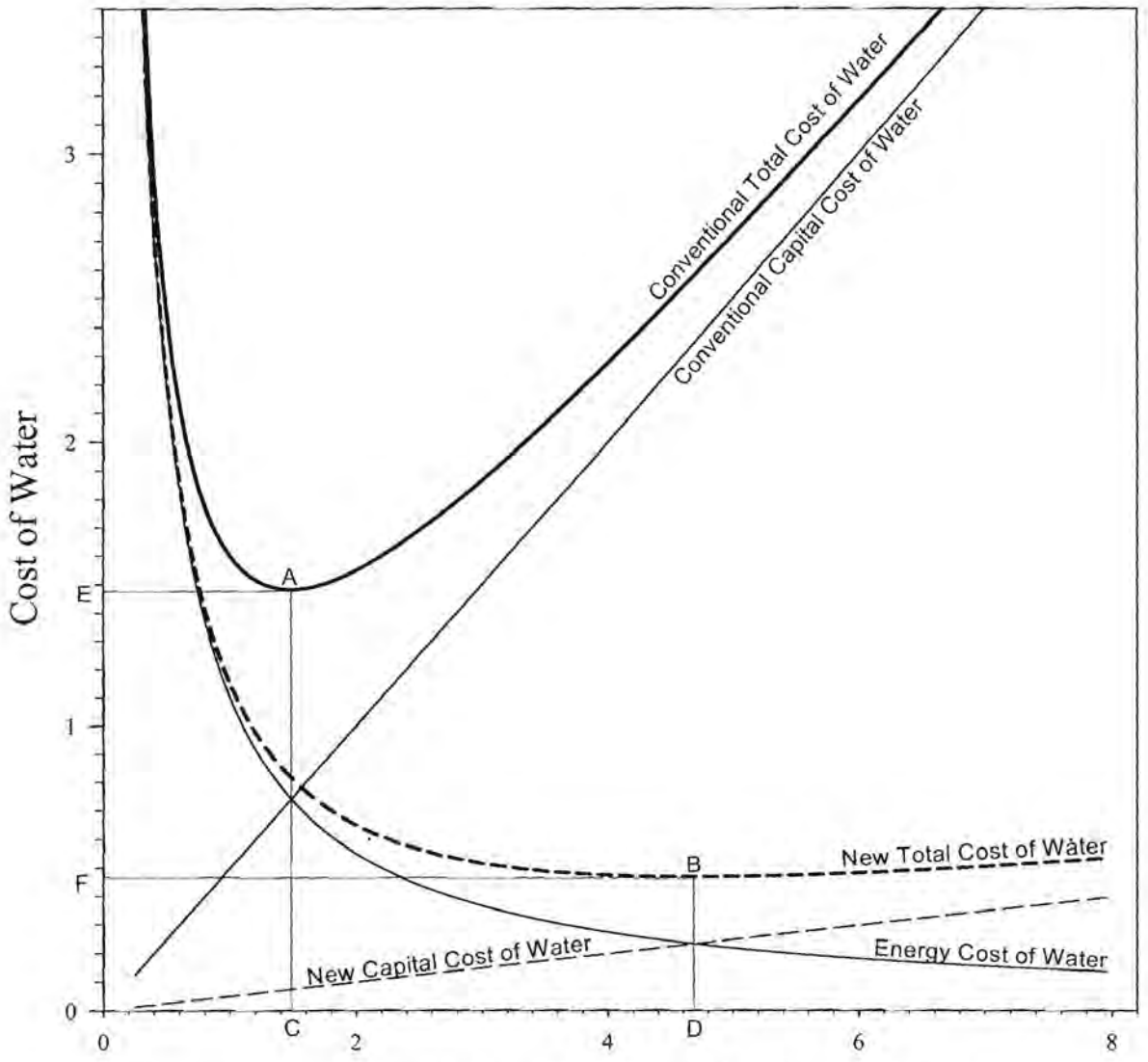

Fig 2.1 Variation of the capital, energy and total cost of desalinated water with the total installed thermal conductance UA. The optimal amount of conductance (point C for the total cost solid curve, and D for dotted one) is that which minimizes the total cost of water. Solid lines are for conventional heat transfer surfaces (high cost per unit conductance). Dashed lines are for thin polymer heat transfer surfaces, where the cost per unit of thermal conductance UA is decreased by more than an order of magnitude. (Of course the cost of the shell will *initially* not show such a dramatic decrease.)

As the unit cost of the conductance decreases, the optimum point A moves down and to the right, to B. More conductance is installed - point C moves to D. The energy consumption and cost decreases, as does the *total* capital cost and the water cost (point E moves to F). In the simplest model: if the *total* capital cost per unit conductance should *decrease* by a factor 10, the energy use, the total capital cost and the cost of water will all *decrease* by a factor of about 3 (=$\sqrt{10}$). The optimal *amount* of conductance will *increase* by this factor (but its *cost will decrease* by the same factor).

We believe that - with a suitable decrease in the cost of the vacuum vessel (shell) - such a decrease is possible. The *decreased cost of the shell* is expected to be the result of further technological improvements due to the sustained growth of the desalination industry, which itself is (and will remain to be) the result of the sustained growth in the demand for potable water.

(UA value) and the energy, capital and total cost of water from a seawater desalination plant after Howe [5]. With increasing conductance UA the energy cost decreases, while the capital cost increases. The *optimum conductance* is where the *total water cost* is a minimum.

Conventional aluminium brass and cupronickel are expensive materials. Yet an annual corrosion allowance of about 25-50μ must be made for these materials [2], even when flow velocities are *below* 2.1 m/s for AlBr, and *below* 4.0 m/s for 70/30 CuNi. Titanium is even more expensive (about $25/kg), but due to the absence of measurable corrosion or erosion in heat transfer or desalination service [2], it can be used in thinner walls. It is also used in erosive flows – e g in flashing flow, and in the top rows of a horizontal tube MED or VCD, where impingement on CuNi and AlBr causes erosive corrosion.

Both high density polyethylene (HDPE) and polypropylene (PP) resist *ionic corrosion* [12] as well as titanium does, and are commonly used to store and transport the most corrosive chemicals – including strong acids, bases and salts. They also show many times the *abrasion resistance* of steel in a Taber abrasion test [12], and may therefore be expected to have excellent resistance against erosive flows.

Their flexibility and elasticity can be used to counter the *adherence of scale* on surfaces treated for wettability. Untreated surfaces possess a well-known anti-stick property [13] which unfortunately is lost when the surface is made wettable.

The *upper brine temperature* of VCD and MED stills have been decreased in the last 2 decades, to reduce the scaling potential. At these lower temperatures (generally below 65°C) the polyolefins (HDPE and especially PP) retain sufficient strength. Also, when they are suitably stabilized, their free radical mediated oxidation does not present a too serious problem at these temperatures.

Heat transfer elements made from *thin* HDPE or PP film (below 60μ) have a calculated *overall heat transfer coefficient* (U value) that is comparable to that of CuNi or Ti metal tubes, but cost far less. See figure 2.2. Thus the material cost per unit conductance is 3 orders of magnitude below that of 0.6 mm titanium. Such low cost per unit conductance

allows the use of more conductance, which reduces the energy consumption, and the total water cost at the optimal point A. Figure 2.1 also shows the effect of reducing the capital (thermal conductance plus accompanying shell) cost – on both the vertical and horizontal position of the optimum (minimum of the total water cost). And on the energy use at this optimal point A, which now moves to B.

Vapour compression stills using heat transfer elements made from such thin polymer film has been used successfully for a decade in VCD units in several countries for the treatment of chemically aggressive industrial effluent and landfill leachate [8]. Their energy consumption is about 9 kWh/m^3 of distillate [8], against about 24 kWh/m^3 for a comparably sized VCD with titanium heat transfer tubes.

The design of these novel units exhibit much ingenuity. Yet with such a new type of technology, we have reason to believe that this design can be further improved on, to give an even lower water cost and energy consumption [10].

The objective of this thesis is a very ambitious one – to design, build and test such an improved distillation system, that would reduce both energy use and capital cost. To understand the scope of the challenge, it should be taken into account that our budget – below €100 000 – was truly modest compared to the €20 million grant that the developers of the competing system received [15]. Thus we had to undertake many tasks which otherwise might have been out sourced. Without support from the Mechanical and Electrical Workshops of the Physics Department, this would not have been possible

We:

(a) conducted an extensive patent search, in which over 3000 (mainly US) patents were briefly examined (abstracts), about 500 with their drawings, and a smaller number in detail.

(b) identified where the existing thin polymer film desalination technology can be improved on (vapour flow resistance).

(c) designed suitable novel polymer heat transfer elements (hte's).

(d) designed vapour flow manifolds, and the mode of affixing the hte's to them. Had the needed manifolds etc specially made.

(e) designed and built saline water distributing and distillate collecting manifolds.

(f) designed, built, tested and improved many apparatuses for fabricating the polymer film heat transfer elements by welding

(g) designed, contracted, tested and refurbished the sealing surfaces of a 400 mm diameter, 3 m tall vertical vacuum shell of 3 mm carbon steel, with external steel ring reinforcement welded on. With 5 large windows to check the wetting of the originally *hydrophobic* polymer film hte's. Despite the dire warnings of an engineer, it has not collapsed when evacuated. However, the sump (from 20mm PVC) imploded, and was replaced with one made of stainless steel. Thermally insulated this vessel.

(h) specified, co-designed, contracted, waited 2 years for and – after many trials and tribulations – and design changes – eventually successfully tested a turbo-compressor, with a specially made high speed water cooled rotary vacuum seal, specially made (in Germany) high speed ceramic bearings and a special high speed belt drive.

(i) had the hydrophobic polymer film hte's treated for wettability *via* oxyfluorination and through a process of sulfonation of which we were the initiators in South Africa (where others are now also using this process for the surface treatment of polymers). Test rigs were built to evaluate the suitability of the treated film for desalination, which requires a *water film* to cover the entire outer surface of the *polymer* film heat transfer element. The results from this testing were correlated with those from contact angle measurement.

(j) assembled the VCD, and successfully tested the integrity of the vacuum system. In addition to the items already mentioned, this required a specially designed and built feedwater heater, pneumatically operated diaphragm pumps for brine recirculation and for distillate extraction, a vacuum pump, and a small plate heat exchanger serving as condenser (cooled with ice water) to protect the vacuum pump from excessive moisture.

2.2 Polymer Heat Transfer Elements

Figure 2.2 shows the calculated variation of overall heat transfer coefficient U in multi-effect distillation with the wall thickness t for a variety of metals and polymers.

The combined effect of evaporative and condensing heat transfer coefficients (plus fouling) was estimated to be about 4400 W/m^{2}K. Despite being poor thermal conductors, polymers of 15-50μ thickness show U-values that are about 60-100% of the value for

titanium or cupronickel used at their traditional thickness (dictated by their rate of corrosion).

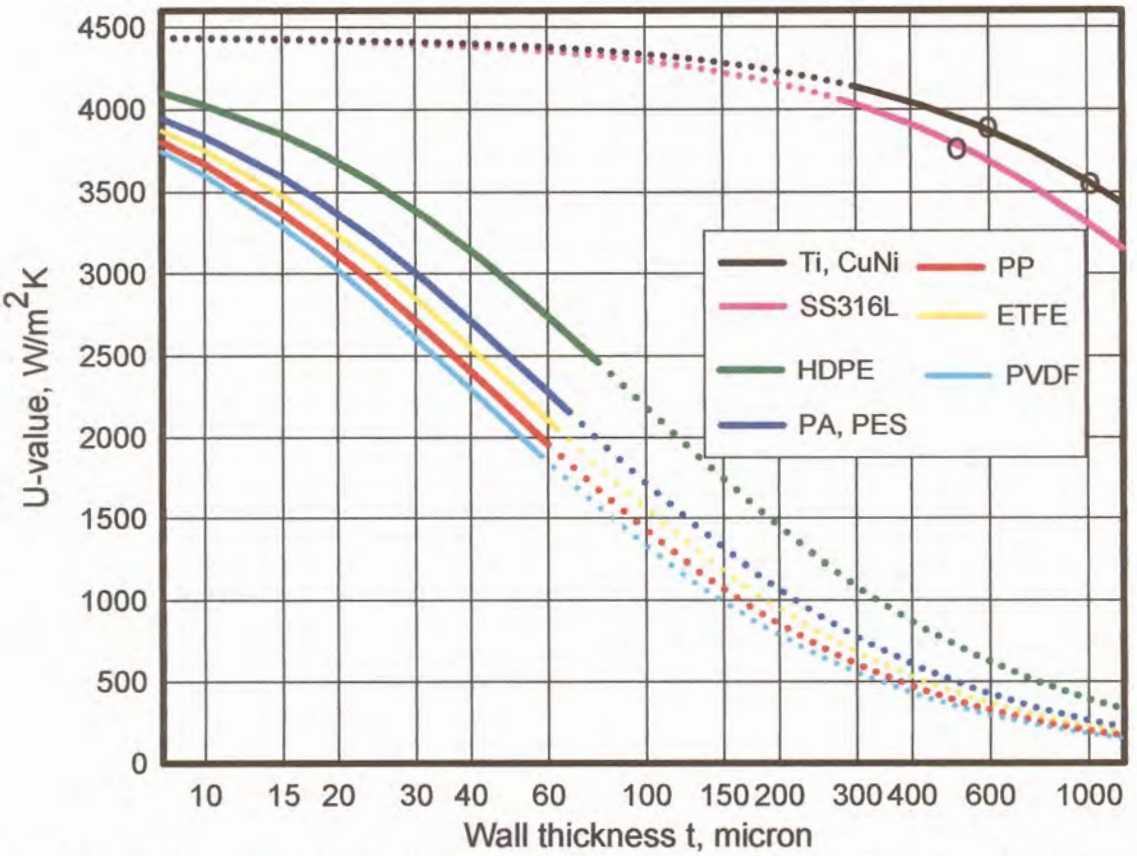

Fig. 2.2 Overall heat transfer coefficients U in MED or VCD as function of wall thickness t for some metallic and polymeric materials. Calculated from $1/U = 1/h_c + 1/h_e + f + t/k$, with the sum of the first 3 terms on the right = 1/(4400) m^2K/W. PA = polyamide, PES = polyester, PVDF = poly(vinylidene fluoride), ETFE = poly(ethylene-tetrafluorethylene).

Thus titanium has normally been used 0.6mm thick, cupro-nickel 1-1.2mm and the rarely used 316L stainless steel 0.5mm. Polyolefins can be used below 30µ. Thus 40µ polyethylene (HDPE) or 20µ polypropylene (PP) give U-values of 3150 – 82 % of the value of 600µ titanium (Ti – 3850 W/m^2K). The material cost of 20µPP is a factor 1000 below that of 600µ titanium. This allows lower energy, capital and maintenance (corrosion & scale) cost. 14µ HDPE gives a U-value *equal to* the value of 600µ titanium.

2.3 Coaxial Helical Polymer Tube Condenser for Multi-stage Flash Distillation – an early project

Multistage flash distillation (MSF) has been the most used distillation process in large scale seawater desalination. For best energy efficiency and best heat exchange efficiency, among others, the number of stages required has to be very high (about 200 stages). Such

a large number of stages required for best energy efficiency presents a limitation to the application of MSF.

Therefore we proposed a modification to conventional MSF. Thin walled (0.5 mm) extruded HDPE tubes were to be used instead of metals as heat transfer surface. The number of stages was to be drastically reduced without sacrifice of the energy or heat exchange efficiency by creating a continuous controllable counterflow temperature gradient within each condenser stage. The vapour flow resistance in each condenser was to be adapted for establishing and maintaining a continuous gradient of saturated vapour pressure, and hence of vapour temperature. Thus, the stage to stage vapour temperature was to be eliminated.

A series of (vertical axis) coaxial helices of HDPE/PP tubing was to form the counter flow condenser. The brine was to flow inside each tube in an upward helical path, while the water vapour and the condensate were to flow outside the tube in a downward direction. With this arrangement, the counter flow nature of the overall flow between the brine and the water was combined with the cross flow nature at local level. The former effect was to maintain an approximately constant temperature difference thus promoting an even and efficient use of the heat transfer surface. The latter effect enhanced the vapour-to-tube heat transfer by generating frequent changes in the vapour flow direction around the tubes.

Using well known formulae from the literature for flow across tube banks the flow resistance in the vapour phase was engineered. The optimal inter-tube spacing and the pressure drop in different parts of the condenser as function of various parameters were determined.

The obtained inter-tube spacing was extremely small and varied along the length of a helix – being smallest (±2.8μ) at the high temperature end and much larger (±40μ) at the low temperature end. This was because of the higher required per stage saturated vapour pressure drop at high temperature, and the higher specific vapour volume at low temperature.

The extreme smallness of the needed inter-tube spacing coupled with the much larger thermal expansion of the diameter of the used tubes caused us to abandon this approach.

2.4 Summary

To further reduce the cost of desalinated water, we develop a vapour compression still with thin film polyolefin (HDPE or PP) heat transfer elements. This will dramatically

reduce the cost of the heat transfer surface – per unit area A, and per unit of conductance. The much lower cost per unit of conductance UA enables the use of more thereof, whereby both the capital and the energy cost of desalinated water will be reduced substantially.

2.5 References

1. K. Wangnick, *2002 IDA Worldwide desalination plants inventory*, Report no. 17.

2. E. Ghiazza and P. Peluffo, *A new design approach to reduce water cost in MSF Evaporators*, Proceedings of IDA conference, Paradise Island, Bahamas, 2003.

3. V. Baujat and T. Bukato, *Research and development towards the increase of MED units capacity,* Proceedings of IDA conference, Paradise Island, Bahamas, 2003.

4. H. Glade, The Carbonate System in MSF Distillers, Proceedings of IDA conference, Manama, Bahrain, 2002.

5. E. D. Howe, *Fundamentals of water desalination*, Marcel Dekker, New York, 1974.

6. C. Sommariva, H. Hogg, and K. Callister, *Forty-year design life: the next target material selection and operating condition in thermal desalination plants*, Desalination 136 (2001) 169-179.

   Also (same authors), *Cost reduction and design lifetime increase in thermal desalination plants: thermodynamic and corrosion resistance combined analysis for heat exchange tube material selection,* Desalination 158 (2003) 17-21.

7. A. Porteus , *Saline Water Distillation Processes*, Longman, London, 1975.

8. Hadwaco brochure, *A quantum leap toward Effluent-Free Industrial Plants*.

9. A. F. Mills, *Heat and Mass Transfer*, Irwin, Chicago, 1995.

10. T B Scheffler, *A cost-effective multi-effect desalinator*, Proceedings of IDA conference, Paradise Island, Bahamas, 2003.

11. A. Macoun, *Alleviating Water Shortages - Lessons from the Middle East*, Desalination & Water Re-use 10/2 (2000) 14 - 20.

12. Hoechst Plastics, *Hostalen*, June 1976.

13. C. Maier and T. Calafut, *Polypropylene: The definitive user's guide and databook*, PDL, New York, 1998.

14. R.S. Silver, *Seawater Desalination:* In Desalination Technology : Developments and Practice, Edited by A. Proteous, Applied Science Publishers, London, 1983.

15. P.R. Koistinen, *Treatment of Industrial Effluents and Landfill Leachates using new low cost Evaporation Technology with Polymeric Heat Transfer Surfaces,* Proc WAT98 - Advanced Wastwater Treatment, Recycling & Reuse. Milan 14-16 September 1998.

3 Flow in a Thin-walled Polymer Tube

3.1 Introduction

In previous chapters we discussed the use of air mattress-like heat transfer elements fabricated from thin flexible high density polyethene (HDPE) and polypropene (PP) film.

In this chapter we show how one may calculate an important design parameter – the diameter of the tubes – as a function of the *fractional* drop $\Delta T_f/\Delta T_1 \equiv 1/R_T$ of the temperature difference along the length of the tubes due to the *frictional* drop Δp_f of the vapour pressure.

We determine the tensile stress in a tube resulting from a pressure difference between the inside and outside of an air mattress-like element, and compare the results with polymer material data [3,4,12].

3.2 Polyolefins (HDPE and PP)

A polymer comprises large molecules – so-called macromolecules. Each of these contains a large number of the same repeating units (monomers) joined by covalent bonds. Synthetic polymers are prepared by polymerization of monomers – which can be by addition or by condensation. The polymerization reaction is mediated by a catalyst [11] and comprises the following stages: initiation, propagation, and termination.

The number n of repeating units is called the *degree of polymerization* (DP).

3.2.1 Polypropene (PP)

Polyprop(yl)ene is a semi-crystalline polymer made by addition polymerization. In the polymerization reaction – in the presence of Ziegler-Natta catalysts – propene molecules are joined together forming a large molecule of polypropene.

$$n CH_2 = CHCH_3 \rightarrow \cdots - [CH_2 - CHCH_3]_n - \cdots$$

Depending on the position of the methyl ($-CH_3$) group on the polymer backbone [9], three possible structures (*stereoisomers*) of PP can be defined:

a) **Isotactic PP:** All methyl groups are located on the same side of the polymer backbone. This is the useful form, which crystallizes in a regular structure, where the pendant methyl groups link adjacent linear chains and imparts good tensile strength and modulus – even at temperatures up to about 100°C. Melting point about 170°C.

b) **Syndiotactic PP:** The methyl groups are alternated regularly between both sides of polymer chain [11].

c) **Atactic PP:** The methyl groups are located randomly with respect to the polymer chain. No crystallinity – an amorphous tarry material.

The catalyst used and the polymerization conditions determine the amounts of isotactic, atactic, and syndiotactic segments in the formulation.

Typical properties of PP are the following:

- low density (about 0.9 g/cm^3)
- good flexibility,
- high stiffness, hardness, and mechanical strength,
- excellent resistance to electrolytes, acids and alkalis.

At high temperatures, in the presence of ultraviolet and ionizing radiation PP decomposes and oxidizes via a free radical chain reaction. The pendant methyl group is especially vulnerable, and is the site of first attack. Stabilizers are added to the melt to counter this degradation. Most are anti-oxidants which act by absorbing free radicals.

3.2.2 High Density Polyethene (HDPE)

High density polyeth(yl)ene is a semi-crystalline plastic developed by Ziegler using low-pressure polymerization. It has a linear molecular structure – with either no branches or a small number of branches – and thus stronger intermolecular forces and more strength than the more branched low density polyeth(yl)ene. In the polymerization process of ethene the double bonds are broken to allow single bonds among the carbon atoms, thus creating a macromolecule – polyethene.

$$n.CH_2 = CH_2 \rightarrow \cdots - [CH_2 - CH_2]_n - \cdots$$

Typical properties of HDPE are:

- low density (0.93 – 0.955 g/cm^3)
- high toughness and tensile strength
- low water absorption
- easily processed and fabricated
- resistant to acids, alkalis, salt solutions, and water
- resistance to temperatures from -50 to 80°C

Special ultra-high molecular mass forms also show resistance to non-polar materials – oils and petrol.

3.3 Optimal Tube Diameter

The diameter of the individual film tubes in an air mattress-like heat transfer element must be carefully chosen, as this choice has important implications for both the capital and the energy cost of a multi-effect or vapour compression desalinator. Thus the choice affects:

(a) the hardware for fabricating the heat transfer elements by multiple line welding.

(b) the design and construction – and cost – of the *entry manifolds for vapour* into the heat transfer elements. A *low vapour flow resistance* is essential for good energy efficiency, and is the primary reason why the existing polymer film desalination technology has only *partly* realized its energy- and capital saving potential.

(c) the *length* of the heat transfer elements that are possible before inner flow resistance to vapour flow in the tubes degrades the energy efficiency. Longer elements will save substantially on the capital cost of the manifolding and of the chambers.

(d) the total size and cost of the *vacuum vessel.* These will be smaller for smaller diameter tubes, which give a higher heat transfer area to vessel volume ratio.

What is needed is a careful balancing/optimization of the capital cost of a smaller vessel, and of longer elements, and of the energy cost benefits of lower flow resistance. For this one needs the pressure drop Δp_f due to the flow as function of:– tube diameter d and length l, temperature difference for heat transfer $\Delta T_1 = \Delta T_0 - \alpha$, overall heat transfer coefficient U; and the density ρ, viscosity μ and enthalpy of condensation L of the vapour.

We now give a simplified derivation of this relation for the case of laminar flow:

Assume

1. *Steady state* operation.
2. The superheat in the vapour is removed. *Saturation* holds inside, and condensation starts at axial position x = 0.
3. *Temperature.* The *outside* temperature T_o is independent of x. *Inside* saturation holds:– the temperature will depend on the vapour pressure p_v, and will decrease when flow resistance causes a decrease in p_v. The temperature difference $\Delta T_1 = T_i(x) - T_o$ between the inside and outside of the tube will also decrease when flow resistance causes a decrease in p_v.
4. The specific volume of the liquid (condensate) is negligible when compared to the vapour. For water at 50°C the respective values are 0.001 and 12 m^3/kg – a ratio of 1 to 12 000. Consequently, for vapour flow we ignore the additional flow resistance due to the presence of the condensate.
5. *Film condensation* inside (as the polymer grade – with a minimum of waxy additives and oligomers – is not *sufficiently* hydrophobic to ensure drop condensation. Dropwise condensation will also not lead to nearly *as* high condensation coefficients with thin polymer film tubes as for metal tubes, where sideways conduction in the wall plays a key role). *Film evaporation* on the outside of the tube, where the surface is treated to make it wettable.
6. The tube *wall thickness t is small* compared to its diameter d: t/d « 1 (3.1a)

   $$\Rightarrow \frac{1}{U} = \frac{1}{h_o} + \frac{1}{h_i} + \frac{t}{k} \qquad (3.1b)$$
7. Because of (3.1a) and the low conductivity of the thin tube wall, we consider only *radial heat conduction* through the tube wall. Also, the very *low axial temperature gradient* further permits us to ignore axial conduction in the wall, in the vapour and in the condensate.
8. All the vapour condenses in a length *l* of tube where the *temperature varies by only 0.1-.5°C.* Therefore the *latent heat* L of condensation, and the *viscosity* μ and *density* ρ of the vapour do not depend on x. Likewise, $\frac{dp_{sat}}{dT}$. The salinity of the brine on the outside tube wall is independent of x.
9. $p_v = p$: *no non-condensibles.*
10. Laminar flow.

A reasonable first approximation is to assume a heat flux and a condensation rate independent of the axial position x. The vapour mass flowrate $\dot{m} = \rho \dot{V}$ will then be a linearly decreasing function of x. From the Poiseuille equation, so will the pressure gradient be. But to simplify the derivation, we first calculated with an $\dot{m}$ that is independent of x, and finally compensated by using (as the mean value) half the value at entrance. The linearity of the Poiseuille equation ensures the correct result from such a simplified procedure.

Heat rate & condensation/evaporation rate

$$\dot{Q} = \mathrm{U}\,\mathrm{A_h}\,\Delta\mathrm{T_l} = U l \pi d \Delta\mathrm{T_l} = \dot{m} L = \rho \dot{V} L \quad \Rightarrow \quad \dot{V} = \frac{U l \pi d \Delta\mathrm{T_l}}{\rho L} \tag{3.2}$$

Poiseuille $$\dot{V} = \frac{\pi R^4}{8\mu}\frac{\Delta p_f}{l} = \frac{\pi d^4}{128 \mu l}\Delta p_f \tag{3.3}$$

Solve (3.3) for Δp_f, and substitute $\dot{V}$ from (3.2): $$\Delta p_f = \frac{128\, U l^2 \Delta\mathrm{T_l}\,\mu}{\rho L\, d^3} \tag{3.4}$$

For U = 2500W/m²K, l = 4m, ΔT_l = 1K, d = .01m, μ from [8] table A4, p702, (3.5)

$$\Delta p_f = \frac{128\times 2500\times 16\times 1\times 1.02\times 10^{-5}}{\rho\times 2.3\times 10^6\times 10^{-6}}\left(\frac{T+273}{293}\right)^{1.15} = \frac{22.7}{\rho}\left(\frac{T+273}{293}\right)^{1.15} \tag{3.4a}$$

Reynolds $$Re = \frac{\rho d v}{\mu} = \frac{\rho d\, 4\dot{V}}{\mu \pi d^2} \overset{(3.2)}{=} \frac{4\, U l \Delta\mathrm{T_l}}{L\mu} = \frac{4\, U l \Delta\mathrm{T_l}}{L\times 1.02\times 10^{-5}}\left(\frac{293}{273+T}\right)^{1.15} \tag{3.6}$$

For the values in (3.4a)& (3.5), $Re = 1705\left(\frac{293}{273+T}\right)^{1.15}$ and the flow is laminar, so that use of Poiseuille's eq (3.3) may be justified. But if $U l \Delta T_l$ should increase more than 35%, this will be a dubious assumption, as the nature of the flow *at the entry to the tube* will then be uncertain (the flow velocity v, like the mass flowrate, will decrease linearly with x).

Let $\Delta p_f = \frac{dp_{sat}}{dT}\cdot\Delta\mathrm{T_f} \equiv p'_{sat}(\mathrm{T})\,\Delta\mathrm{T_f}$, where ΔT_f is the drop in saturation temperature due to the pressure drop Δp_f. With this into eq (3.4),

$$d^3 = \frac{64\, U l^2 \Delta\mathrm{T_l}\,\mu}{\rho L\,\Delta p_f} = \frac{64\,\mu\, U l^2\,\Delta\mathrm{T_l}}{\rho L\; p'_{sat}(\mathrm{T})\;\Delta\mathrm{T_f}} \tag{3.7}$$

will give the design diameter as a function of the parameters mentioned at the outset. To include the linear decrease (to 0) of $\dot{m}$, the factor 128 has been halved. An independent derivation of (3.7) (or of (3.4) with 128 halved) can also be given. It is more complex, and will not be included here.

It appears from the important result (3.7) that the optimal tube diameter depends on the *fractional drop* $\Delta T_f/\Delta T_l$, the ratio between the temperature difference along the length of the tubes due to the *frictional* drop $\Delta p = \Delta p_f$ of the vapour pressure, and the temperature difference between the inside and the outside of the tubes. The derivation (in which ΔT_l is treated as independent of x) is valid as long as this fraction is small. That is, as long as its inverse, the *ratio*

$$R_T = \Delta T_l/\Delta T_f \text{ is } >>1. \tag{3.8}$$

Figures 3.1 - 3.6 show the diameter d calculated from (3.7) for 2, 4 and 8m long 50μ thick polypropene (PP), where according to fig 2.2, U = 2500 W/m² K. Also for similar lengths of 39μ thick polyethene (HDPE), where U = 3200 W/m² K. For values 3, 4, 5, 6, 8 and 10 of the ratio R_T (i.e. for a fractional pressure drop $\Delta p_f/\Delta p_l$ of 1/3, 1/4, 1/5, 1/6, 1/8 and 1/10). For the temperature range (35 - 90°C) relevant for polyolefin film heat transfer elements.

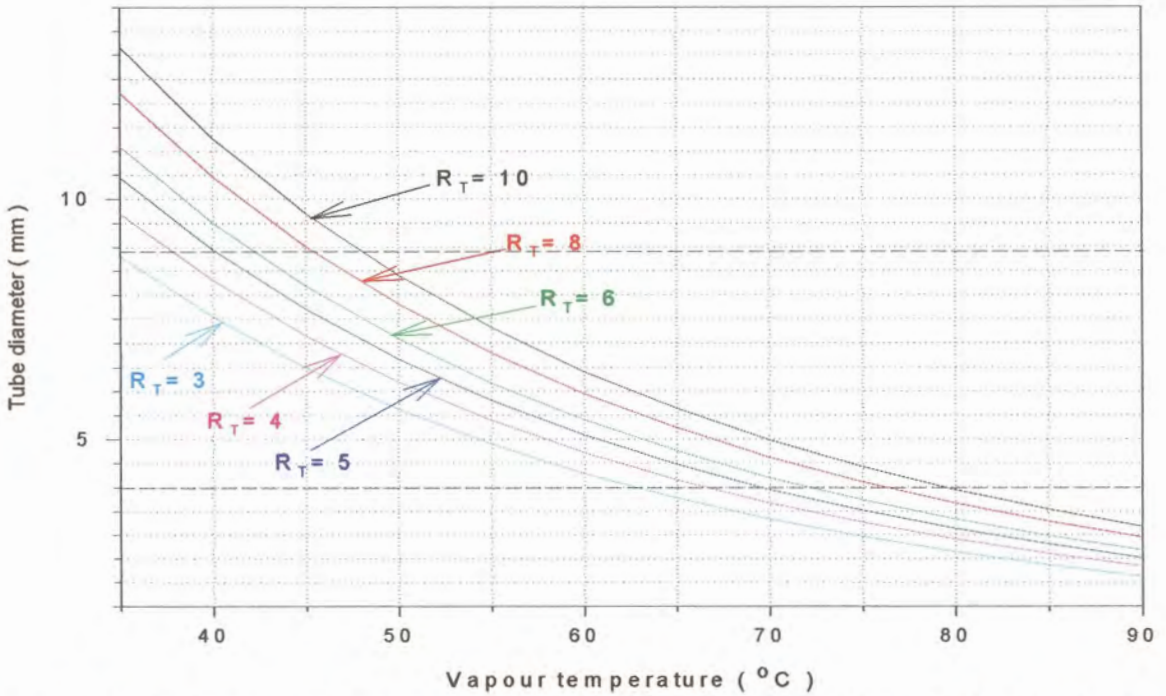

Fig. 3.1 Tube diameter as function of temperature for given ratios R_T (eq.(3.8)). For 2 m long tubes of 50μ thick PP film (U value 2500W/m^{2}K). The dashed horizontal lines indicate tube diameters that can be readily produced by our film welding apparatus.

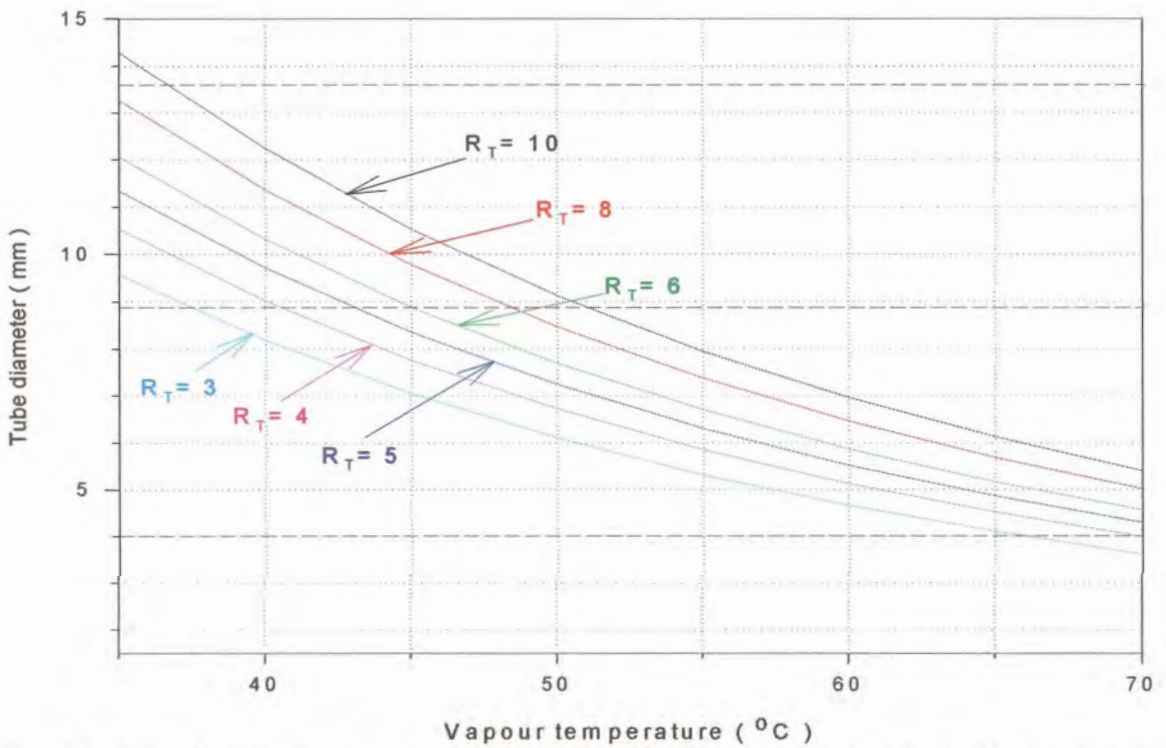

Fig. 3.2 Tube diameter as function of temperature for given ratios R_T (eq.(3.8)). For 2 m long tubes of 39μ thick HDPE film (U value 3200W/m^{2}K).

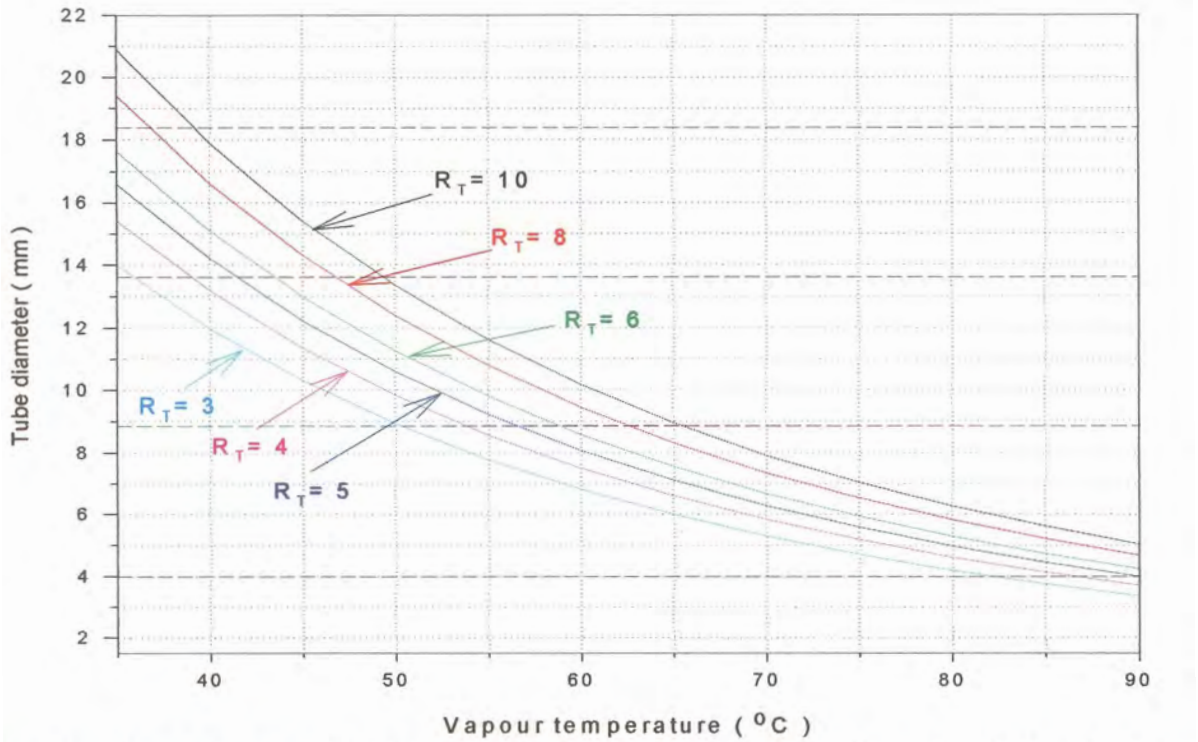

Fig. 3.3 Tube diameter as function of temperature for given ratios R_T (eq.(3.8)). For 4 m long tubes of 50μ thick PP film (U value 2500W/m^{2}K).

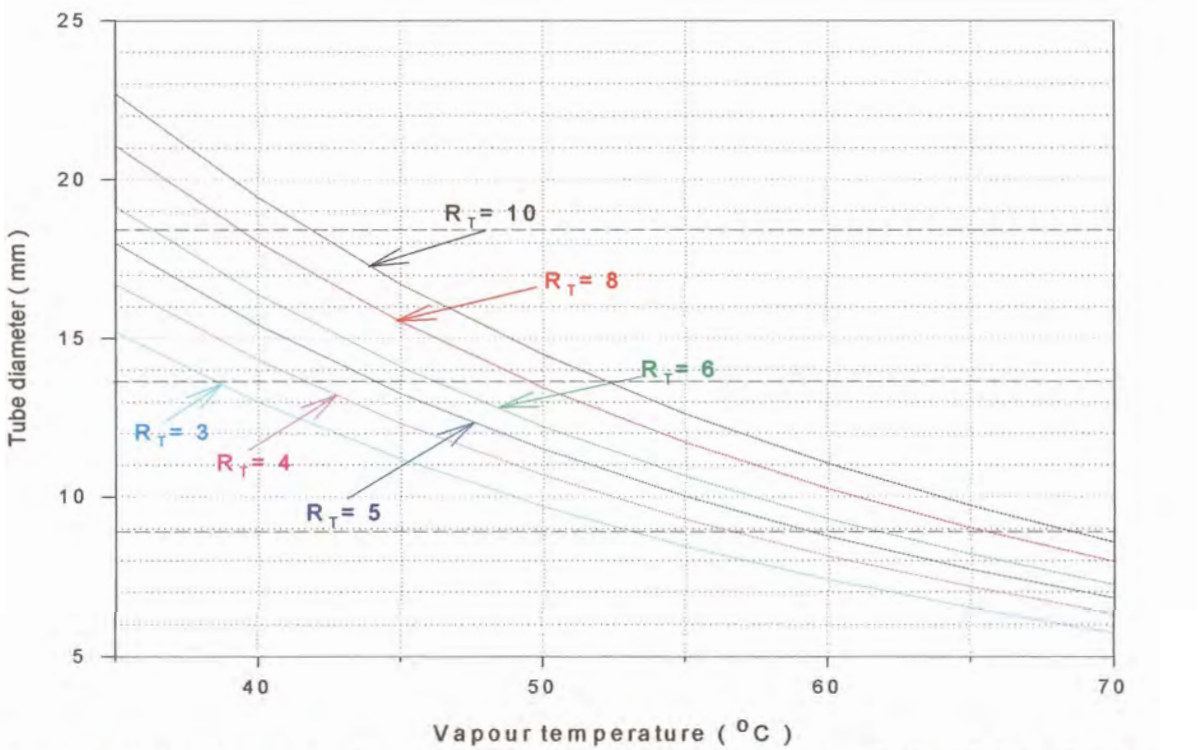

Fig. 3.4 Tube diameter as function of temperature for given ratios R_T (eq.(3.8)). For 4 m long tubes of 39μ thick HDPE film (U value 3200W/m^{2}K).

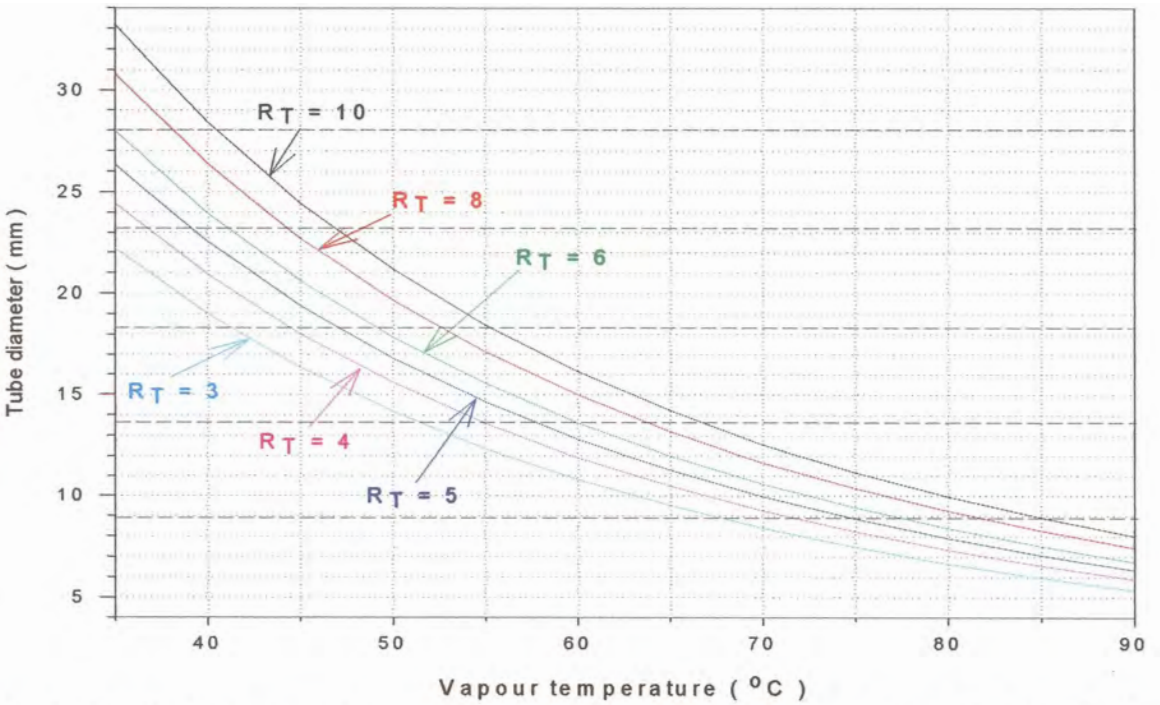

Fig. 3.5 Tube diameter as function of temperature for given ratios R_T (eq.(3.8)). For 8 m long tubes of 50μ thick PP film (U value 2500W/m^{2}K).

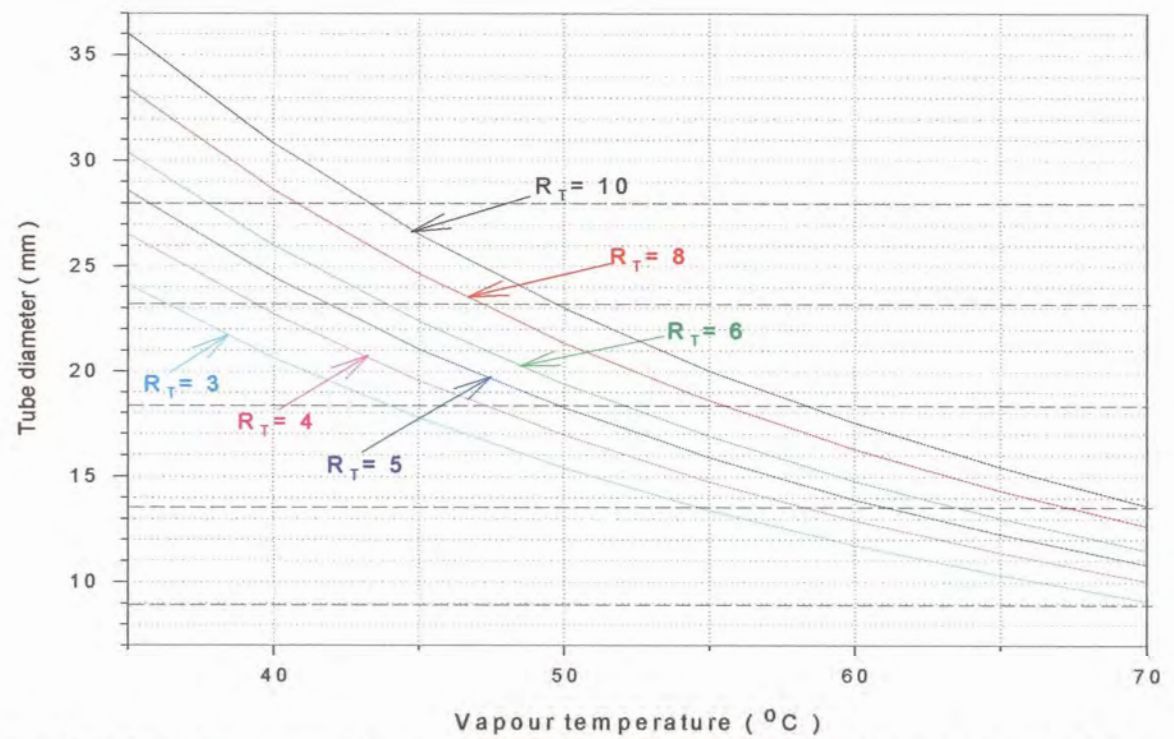

Fig. 3.6 Tube diameter as function of temperature for given ratios R_T (eq.(3.8)). For 8 m long tubes of 39μ thick HDPE film (U value 3200W/m^{2}K).

As seen from these figures, the tube diameter d decreases with increasing temperature T. In eq (3.7) this follows from the dependence $\rho(T)\, p'_{sat}(T)$. The reduction is steeper at lower temperatures. For given T, d decreases with increasing fractional drop in temperature difference, and increases with its inverse – R_T.

3.4 Tensile Stress in Polymer Film Tubes. Creep

Polymers are *visco-elastic* materials. When subjected to an applied stress, they behave partly as fluids of very high viscosity and partly as elastic solids. Thermoplastics, in particular, exhibit a behavior known as *creep* which is the deformation of the material in the course of time under constant load. In all thermoplastics, creep rupture strength falls off as the duration of the applied stress is lengthened. This can happen even at room temperature and under relatively slight load stress.

In quantitative design involving polymers the visco-elastic effects must be considered [8]. In the present case the plastic tube is subjected to a tensile stress σ due to the pressure difference between the saturated vapour (inside) and the lower pressure vapour on the tube's outside surface. This stress acts uniformly in the directions orthogonal to the wall. It induces a tensile strain which depends on the stress as well as the applied time. The tensile stress in a tube of diameter d and wall thickness t under pressure difference Δp is given by

$$\sigma = \frac{\Delta p d}{2t} . \qquad (3.9)$$

The vapour pressure difference Δp between the inside and outside of the polymer film tube includes a term $\Delta p_1 = p'_{sat}(T)\, \Delta T_1$ for the pressure difference needed to create a temperature difference ΔT_1 for heat flow. And another term $\Delta p_{saline} = p'_{sat}(T)\, \alpha$ representing the reduced pressure outside the tube due to the salinity of the evaporating brine. Here α is the boiling point elevation due to the salinity of the evaporating brine. Therefore the total pressure difference Δp in (3.9) is

$$\Delta p = \Delta p_1 + \Delta p_{saline} = p'_{sat}(T)\, \Delta T_0 \qquad (3.10)$$

where $\Delta T_0 = \Delta T_1 + \alpha$ is the per effect temperature difference in a multi-effect plant. In a vapour compression plant Δp is the pressure difference created by the compressor.

The tensile stresses were calculated for the tube diameters corresponding to $R_T = 8$ (a fractional drop in temperature difference of 1/8) – for $\Delta T_0 = 2K$ with 2, 4 and 8 m long 50μ thick PP and 39μ thick HDPE film tubes. According to equations (3.9) and (3.10) the tensile stress – plotted in figure 3.7 – increases with the temperature. This is because the slope p' of the vapour pressure curve increases steeply with T – more than offsetting the reduction of d with increase in T.

The tensile stress values shown in fig 3.7 are below 0.4 MPa. For (a suitable grade of)

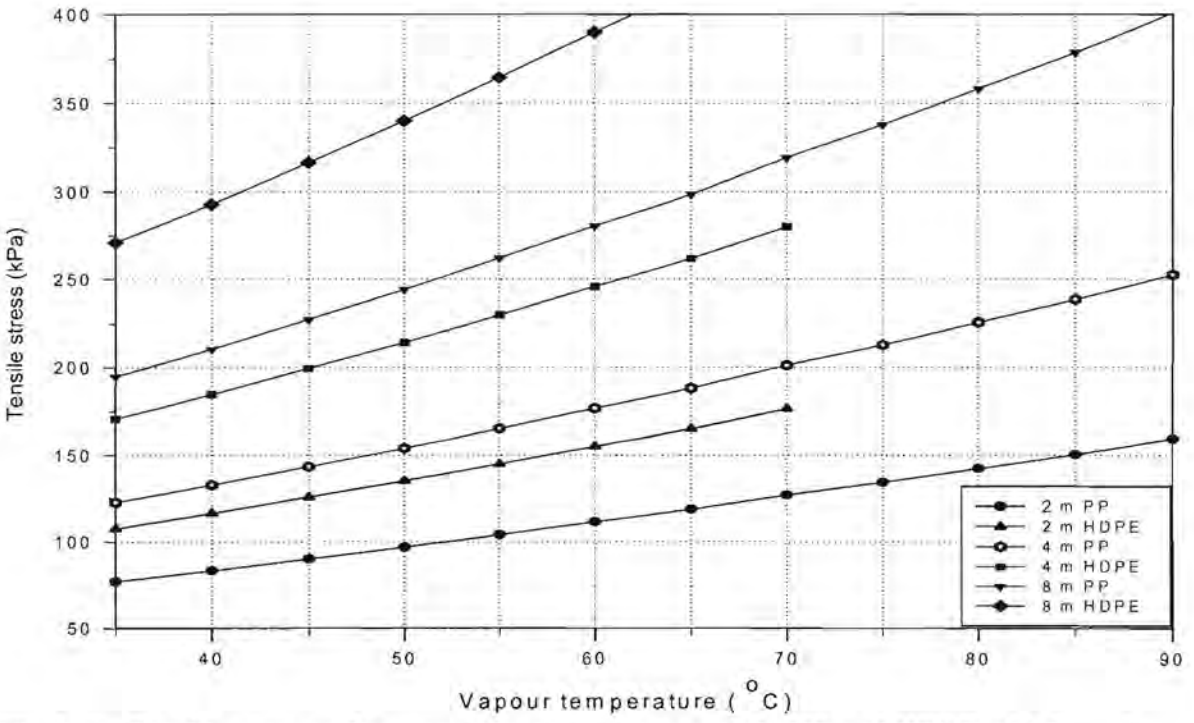

Fig. 3. 7 Tensile stress as function of vapour temperature for PP and HDPE with $R_T = 8$.

polypropylene the creep data [3,12] show that it can handle – with minimal (~ 1%) creep – a tensile stress of 7.7 MPa at 40°C, 5 MPa at 60°C, and about 2MPa at 80°C – for 10 years. At 95 - 100°C it can likewise handle ~ 2 MPa for 1 year. Therefore, polypropylene appears to have sufficient tensile creep strength to be used as film tube material in thicknesses far below the 50μ we have so far considered. Indeed, at 10 or 15μ it would still probably have sufficient creep strength (and a much better U value than at 50μ), if at this low thickness it can still be suitably welded and made wettable. Polyethylene [4] appears able to handle a tensile stress of 3.5 MPa at 40°C for 10 years, and 2.2 MPa at 60°C for 1 year. Extrapolation suggests 0.5 MPa at 60°C for over 10 years.

A good choice will be to choose PP over HDPE above about 60 - 65°C (higher for shorter film tubes, lower for longer ones). If it is deemed best to go to temperatures above 90°C, then it will be best to use a fluoropolymer such as ethylene-tetrafluor-ethylene (ETFE), poly-(vinyl fluoride) (PVF) or poly-(vinylidene fluoride) (PVDF).

An advantage of going above 90°C would be to operate close to atmospheric pressure, which will save on the considerable cost of a vacuum vessel and of vacuum pumps and vacuum pumping. However, one needs also to consider the very substantial extra cost of the more expensive polymers, and of their more expensive wettability treatment.

3.5 Summary

Equation (3.7) (and the figures (3.1) to (3.5)) relate the tube diameter d to temperature and the fractional drop $1/R_T$ in temperature (due to frictional pressure drop). This relation is essential for optimizing the film tube dimensions (length, diameter and thickness) for the air mattress-like heat transfer elements.

The tensile stresses for $R_T = 8$ are below 0.5 MPa for polypropylene (PP), and for HDPE below 65°C . Up to about 60 - 65°C high density polyetylene (HDPE) has sufficient creep strength, and up to about 95°C, PP also has sufficient creep strength to be used as film tube material as described herein.

3.6 References

1. K Wangnick, *Present status of thermal seawater desalination techniques*, Desalination and water Re-use 10/1 (2000) p14-21.
2. C. Hall, *Polymer Materials: An Introduction for Technologist and Scientists*, Macmillan, 1986.
3. Hoechst Plastics, *Hostalen PP*, July 1976, fig. 8.
4. Hoechst Plastics, *Hostalen*, June 1976, fig. 7.
5. A. F. Mills, *Basic Heat and Mass Transfer*, Irwin, Chicago, 1995.
6. S.P. Sukhatme , *A textbook on Heat Transfer*, Orient Longman, Hyderabad India, 1989.
7. R. S. Silver, *Seawater desalination,* In: Desalination Technology Ed A Porteous Applied Science Publishers, 1983.
8. N. G. McCrum, C. P. Buckley, and C. B. Bucknall, *Principles of Polymer Engineering*, Oxford University Press, New York, 1997.
9. F. M. White, *Fluid Mechanics*, McGraw–Hill, New York, 1994.
10. Kirk-Othmer, *Encyclopedia of chemical technology – Nickel and Nickel Alloy to paint*, 4th edition, Volume 17, John Willey & Sons, New York.
11. O. Schwarz, *Polymer Material Handbook*, Translated from German by F.-W Ebeling,

H. Schirber, H. Huberth and N. Schlör, for the Plastics Industry Training Board (PITB), South Africa, 1995.

12. C. Maier and T. Calafut, *Polypropylene: The definitive user's guide and databook*, PDL, New York, 1998.

List of Symbols

A_h : total area for heat transfer (m^2)

d : diameter of heat transfer tube (m)

h_i : condensation coefficient inside film tubes (W/m^2K)

h_o : evaporation coefficient outside film tubes (W/m^2K)

k : conductivity of polymer film heat transfer material (W/mk)

L : enthalpy of evaporation (J/kg)

$\dot{m}$: mass flow rate of vapour (kg/s)

p : pressure of vapour + non-condensible gases (Pa)

p_v : vapour pressure (Pa)

q : heat flux (W/m^2)

$\dot{Q}$: outward heat flow rate through tube wall (W)

R_T : ratio between the temperature difference between the inside and the outside of the tubes, and temperature difference along the length of the tubes due to the *frictional* drop Δp_f of the vapour pressure (-)

t : thickness of polymer film tube wall (m)

T : temperature (K or C)

U : overall heat transfer coefficient (W/m^2K)

v : vapour flow velocity (m/s)

$\dot{V}$: vapour volume flowrate (m^3/s)

x : axial position along tube (m)

α : boiling point elevation of evaporating saline water on outside of tubes (K or C)

Δp : pressure difference between inside and outside of polymer film tubes (Pa)

Δp_f : pressure drop due to friction inside tubes (Pa)

Δp_i : pressure difference needed to create a temperature difference ΔT_i (Pa)

Δp_{saline}: reduced pressure outside the tube due to the salinity of evaporating brine (Pa)

ΔT_1 : temperature difference for heat transfer between condensing vapour and evaporating saline water In- and outside film tubes (K or C)

ΔT_f : decrease in saturation temperature due to vapour flow resistance (K or C)

$\Delta T_o = \Delta T_1 + \alpha$: temperature difference per effect (K or C)

μ : dynamic viscosity of vapour (kg/ms)

ρ : mass density of vapour (kg/m^3)

σ : tensile stress (Pa)

4 Fabrication of Polymer Film Heat Transfer Elements

4.1 Introduction

The use of inexpensive thin corrosion resistant plastic films as heat transfer elements can reduce both the capital costs and the energy requirement of a distillation system [1, 2]. For the film to be able to withstand the vapour pressure difference between the condensing and evaporating sides we fabricated "air mattress" elements – by welding two superposed plastic films (or 2 parts of a folded single film) together along parallel weld lines.

The process of joining thermoplastics using heat and force is named plastic welding [3]. All welding methods have in common three steps – plasticising, joining and cooling. The quality and strength [3] of a thermal weld are determined by an accurate selection of the welding parameters – welding temperature, welding pressure and temperature effect time. The welding temperature permits the plastic to reach the plasticised state. The welding pressure ensures a close bonding of the joining surfaces, and the correct temperature effect time ensures that the heat reaches a sufficient depth in the parts to be joined.

In this chapter we describe the design, building and testing of the welding apparatus.

4.2 Welding Apparatus (Design)

The final version of the thermal impulse indirect welding [3] apparatus used to weld polymer films is shown in figure 4.1. It comprises a smooth and flat block of polished granite (1100 mm x 320 mm x 30 mm) placed on a table. Two layers of a mica composite material were laid on top of the granite block to reduce heat loss to the granite during welding. At each end of the granite is a block of nylon (320 mm x 30 mm x 30 mm) fitted with 40 brass studs of 8mm diameter. Each stud is designed to clamp and hold the end of a flat nichrome ribbon of the type used as heating elements. In the first configuration, as seen in figure 4.2, the welding apparatus had 40 parallel ribbons – each 1140mm long – used as heating elements. They were placed on a sheet of polytetrafluorethylene impregnated fibreglass cloth on top of the mica layers. In the transverse direction the

ribbons were spaced 7.5 mm centre to centre. When assuming perfect flexibility of the film, this setup permits the fabrication of "air mattresses" with tubes of 4.0 mm diameter.

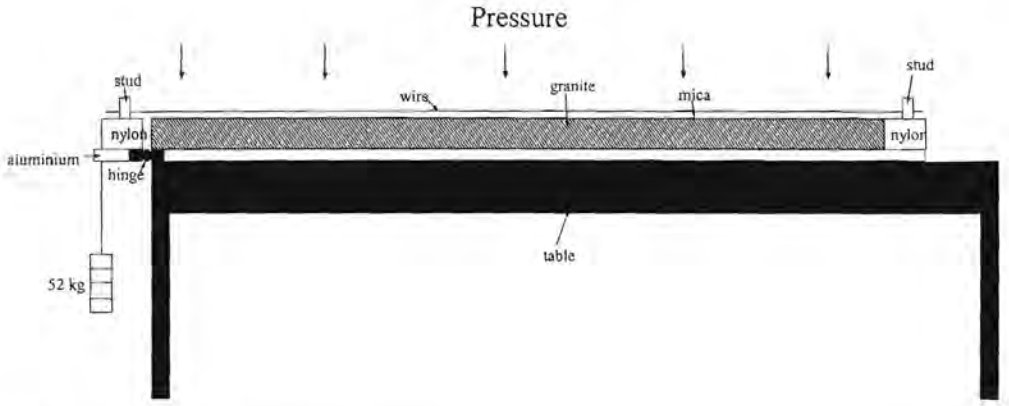

Fig. 4.1 Side view of the welding apparatus.

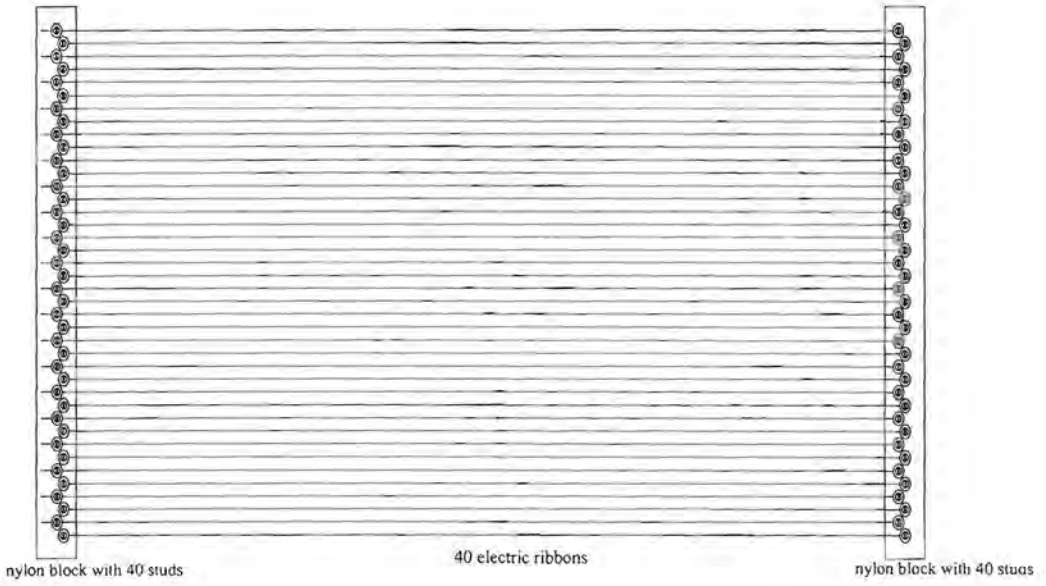

Fig. 4.2 Schematic overview of the first configuration of the welding apparatus with 40 electric heating ribbons. In a later version, only every 4th ribbon was retained.

In later versions the number of ribbons in the apparatus was reduced to 7, 8 or 10. Only every 4th stud was used, so that the new centre to centre spacing was 30 mm, corresponding to "air mattress" tubes of 18.4 mm diameter.

An adapted pocket scale (with its hook replaced by a ribbon clamp) was used to put all ribbons under the same initial tension of 25 N. This procedure was repeated every day welding was carried out.

4.2.1 Heating Elements

For the identification of suitable heating elements to be used in the welding apparatus, round (295, 355 and 560 μ diameter) and flat (794 μ x 254 μ) nichrome wires were tested. Nichrome is a Nickel/Chromium alloy (Ni80%/Cr20%) with a "normal" coefficient of thermal expansion:– $\alpha = 14 \times 10^{-6} K^{-1}$ at 20 - 100°C [8].

The wires – each 1140mm long – were put under variable electrical load in the welding machine to test their weld capability on polypropylene (PP) films of different thicknesses. However the obtained weld lines on the PP films using the round wires were weak. Due to the round shape during welding molten material was squeezed out from the welding zone under the applied pressure. The round wires were therefore excluded and the ribbons were instead adopted as the electrical heating elements for the welding apparatus.

The thermal expansion of the ribbons was of real concern. Thus a practical way to offset the expansion, thereby preventing the ribbons to move sideways and touch one another during welding had to be found. The ribbons were heated with electrical currents from 1 to 5 A. Initially a single ribbon and gradually the number was increased to 3. This was done to establish the effect of the increase of the number of ribbons on the thermal expansion.

Figure 4.3 shows the dependence of the thermal expansion (the mean of two measurements) on the applied power per unit length for the ribbons. As seen from the graph, the thermal expansion increases with the growing electrical heating power. This increase is slightly steeper with a larger number of ribbons. Then the generated heat in a wire contributes not only to its own temperature increase and expansion but also to the temperature increase and thermal expansion of the neighboring ribbons.

In an attempt to use elements with lower coefficient of thermal expansion than nichrome, invar was tested. Invar is a ferromagnetic iron-nickel alloy (64%Fe and 36%Ni) with the

lowest thermal expansion coefficient of its kind (α = 1.7 - 2.0 x $10^{-6}K^{-1}$at 20 - 90°C [8]).

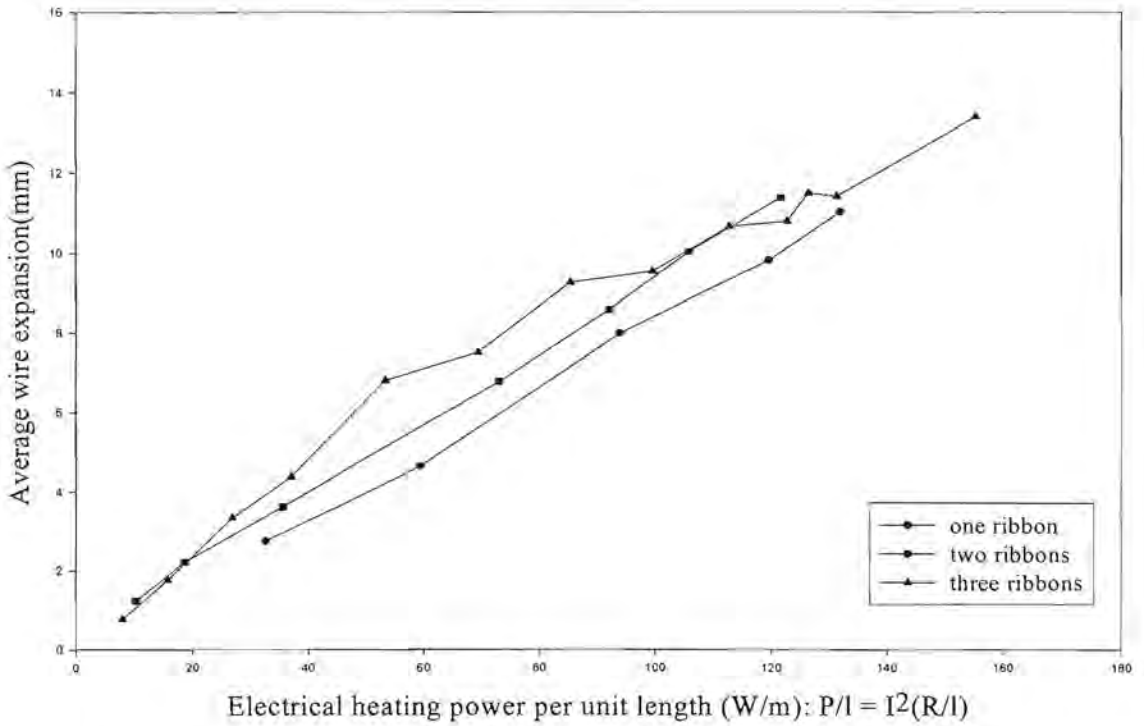

Fig. 4.3 Dependence of thermal ribbon's expansion to the electrical heating power per unit length.

As shown in figure 4.4 invar exhibits a uniform expansion up to near the inflection point – which increases with nickel content. The inflection point is associated with the Curie temperature. Above this temperature the magnetic properties in the material are lost, therefore it expands as much as other metals (slightly more than pure iron – its main constituent).

For welding plastics heat must be transferred from the ribbon to the plastic therefore the ribbons' temperature should be higher than the welding temperature – plasticised state. The used invar ribbons (150μ x.600μ) – specially manufactured for the project – displayed nearly as large thermal expansion as that of nichrome. At a welding current of 2.50A they changed colour due to oxidation. Further attempts at using the oxidized ribbon caused breakage due to embrittlement.

We also thought to use other metals such as molybdenum ($\alpha = 5.1x10^{-6}K^{-1}$) and tungsten

($\alpha = 4.5 \times 10^{-6} K^{-1}$) which have lower thermal expansion than nichrome. However within our budget we could not find ribbons in these materials.

Different approaches were tested to compensate the thermal expansion experienced by the adopted nichrome ribbons. Initially – as shown in figure 4.5 – springs of different strengths were attached to a movable nylon block. The block could slide longitudinally

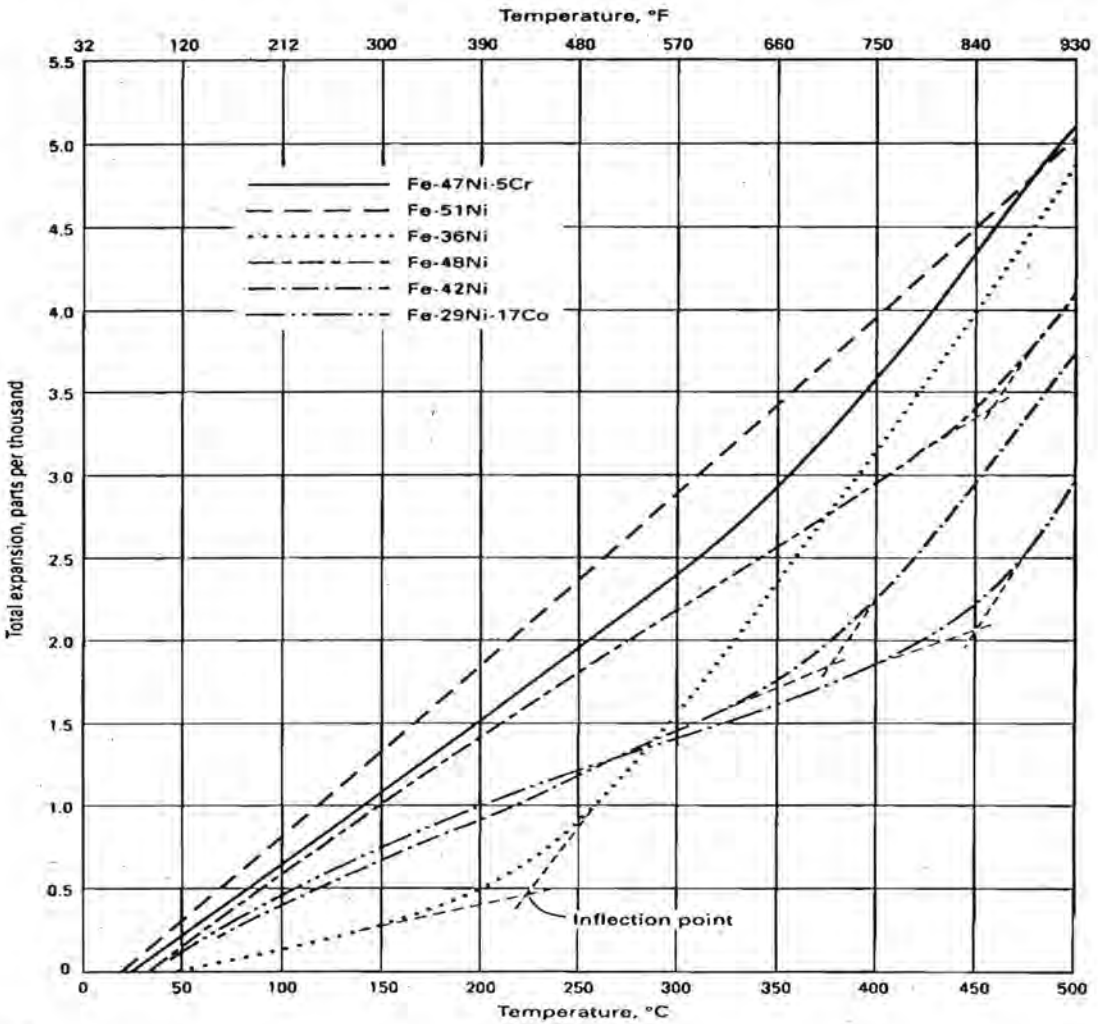

Fig. 4.4 Total thermal expansion of iron-nickel alloys showing the effect of third elements [6].

over 3 brass rods imbedded in the granite slab. During welding the ribbons – attached to the nylon block through studs – expanded thermally. With the help of the springs the nylon block was pulled and in this way the ribbons' expansion was offset. However, friction between the nylon block and brass rods hampered the effective compensation of the thermal expansion.

In another setup – as illustrated in figure 4.1 – weights totaling 52 kg were attached to a thick hinged aluminum plate on top of which a block of nylon was fixed. Three strong door hinges were used to connect the moving part to the granite block. During welding

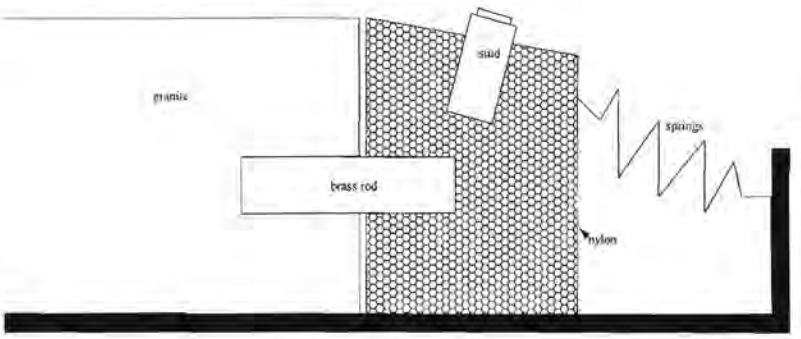

Fig. 4.5 Schematic setup using springs to offset thermal expansion of the used ribbons.

the ribbons' thermal expansion was compensated using the weights for straightening the ribbons. This option was so far the best alternative and was therefore adopted.

4.2.2 Welding Pressure

As mentioned, the weld pressure is an important welding parameter. We built and tested various devices to apply the needed uniform pressure during welding.

The first comprised commercially available sheets of molded foamed silicone rubber (300 x 300 x 10 mm). These were precisely cut and glued on to a piece of flat plywood. Due to the non-uniformity of the thickness and modulus in the silicone sheets the application of a uniform pressure on the welding area was not possible.

In other development a pneumatically inflated thin-walled silicone rubber tube was tested without success. As shown in figure 4.6, fabricated silicone rubber tubes of different wall thickness were confined on 3 sides inside a large rectangular aluminum channel and inflated with compressed air. Weights were placed on top of the frame to exert the pressure during welding.

Yet another pressure device was tested. It comprised a layer of polyether foam rubber glued on to one side of a piece of a flat chipboard. Three 25 kg slabs of granite – placed

on the top side of the chipboard – were used to exert the pressure during welding. With

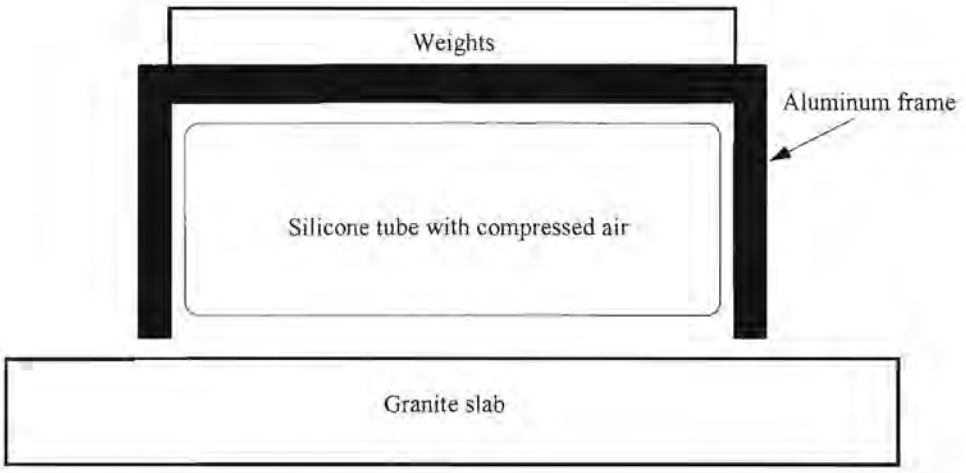

Fig. 4.6 Drawing visualizing the application of weld pressure using pneumatically inflated thin-walled silicone rubber tube.

this option better welds were attained. This alternative was unpleasant due to the need to lift and replace heavy slabs each time a welding had to be carried out.

Financial constraints prevented the use of a more convenient option.

The welding pressure obtained with the adopted option – as seen in table 4.1 – is low

Process	**Welding Pressure (kPa)**
Heated tool [7]	100 - 350
High frequency [7]	500 - 2000
Spin [7]	1000 - 7000
Induction [7]	100 - 300
Resistance implantation [7]	62
Commercial impulse heat sealer (our measurement)	24
Our impulse method	2.3

Table 4.1 Welding pressure for polypropylene used in different technologies.

compared with the pressures proposed in the literature for other techniques. As a result,

a relatively high welding current was used. However, an increase of the welding pressure would lead to higher friction between the ribbons and the films. This could cause the breakage of the films.

4.3 Fabrication of "Air Mattresses"

Commercially available 20, 30 and 50μ thick polypropylene (PP), and later specially made 39μ high density polyethylene (HDPE) films were used to build tubelike elements – the "air mattresses" – to be employed as heat transfer unit in a mechanical vapour compression desalination prototype plant (MVC). The films were welded using the thermal impulse indirect welding process [3].

The welding process started with an electrical circuit comprising 10 ribbons. Several welds were done, using 20, 30 and 50μ thick polypropylene films of different lengths. The welding with 20 and 30 μ films was not satisfactory – especially for films of 1 m long. They were, therefore, abandoned. Thus the 50μ PP films were adopted as the first material to used for the fabrication of the "air mattresses".

The electrical circuit was increased – in steps – from 10 to 40 ribbons. This permitted the fabrication of "air mattresses" with 40 vertical weld lines (1000 mm x 1 mm) spaced 7.5 mm centre-to-centre. Parameters such as current, time, and pressure were deliberately changed – one at a time – until strong welds were attained.

The attainment of suitable welding parameters was a difficult task. It required some patience from the welder. During welding, the current and welding time were recorded against the weld quality. This information served as basis for further tests to improve the welding. The optimal welding parameters found for the 50 μ PP film were 7 seconds weld current time, 3.95 A weld current in each ribbon, and 2.3 kPa weld pressure.

The alternating current electrical power supply to the system was provided by four independent 15A, 230V electrical circuits. Each circuit comprises a variable transformer for the adjustment of the welding current, a multi meter for current or voltage measurement, and two equal resistors in parallel. Each resistor comprises five ribbons – heating elements – connected in series. The four circuits were coupled to a timer used to

set the temperature effect time.

As mentioned in section 4.2, due to practical reasons the configurations of the "air mattresses" was changed. The number of tubes was reduced from 40 to 7 or 10 tubes of bigger diameter. The used electrical circuit in the final version of the welding machine is shown in figure 4.7. Each resistor comprises four ribbons – instead of five – connected in series.

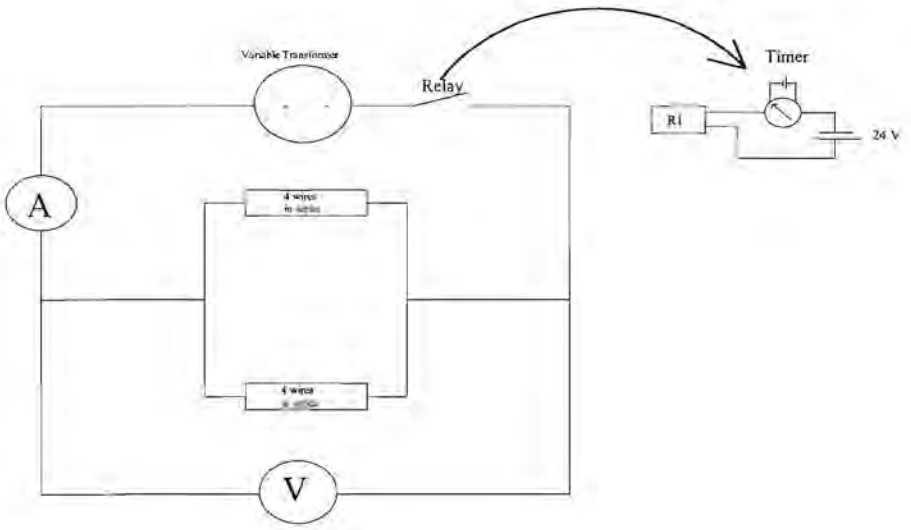

Fig. 4.7 Diagram of the electrical circuit used in the final version of the welding apparatus.

Later, the 39μ HDPE film from a special grade suitable for wettability treatment (see next chapter) was adopted as heat transfer material for the desalinator. It has the advantages of a lower wall thickness and higher thermal conductivity than the 50μ PP film. For this the welding parameters were 3 seconds, 3.9 A and 2.3 kPa.

4.4 Pressure and Leakage Tests

The "air mattresses" produced with the welder showed sound welds. This was confirmed by visual inspection against back light and by inspection with a Nikon 6C-2 profile projector. The strength of the welds in the "air mattresses" with eight tubes were checked using compressed air.

Initially a single tube was inflated with compressed air and gradually the entire "air mattress". Maximum air pressures of 400 kPa for a single tube and 350 kPa for the entire "air mattress" were recorded for the 7.5 mm PP film tube mattresses. In use the pressure difference between the inside and outside of the desalinator will be below 5 kPa. However, at temperatures above room temperature the plastic films become weaker.

For leakage detection some inflated "air mattresses" were introduced inside a container filled with water. The "air mattresses" experiencing air leakages – due to discontinuities on the weld lines – were repaired with a tool built specially for this purpose.

The device – as shown in figure 4.8 – comprises a disk of approximately 40 mm diameter and 16mm thick made of "vesconite" polyester. The round surface is covered with a small sheet of polytetrafluoroethylene impregnated fiberglass cloth. On top of the cloth – in the middle of the disk – a short piece of nichrome ribbon was attached. Both ends of the ribbon were connected to a power supply used to heat the element. A metal rod covered with insulation tape is used as a handle for applying the weld pressure. The electrical power and the weld pressure are manually adjusted for welding weak spots or places with discontinuities in the films.

4.5 Summary

The design and building of the welding apparatus was successful. However, the welding apparatus still needs further improvements to facilitate the process of mass production of the "air mattresses". Thus, the following considerations need to be attended to for the improvement of the apparatus:

(a) The adjustment of the welding current with the adopted electrical setup – in the case where 40 ribbons were used – was done independently in each circuit. With this procedure the application of the same values of current in each circuit was difficult. This resulted in the production of "air mattress" with tubes of different strengths. For safety reasons the electrical setup needs to be compact and well insulated.

(b) The manual procedure for the application of the pressure during welding was arduous. It did not ensure the needed uniformity in the application of pressure across the

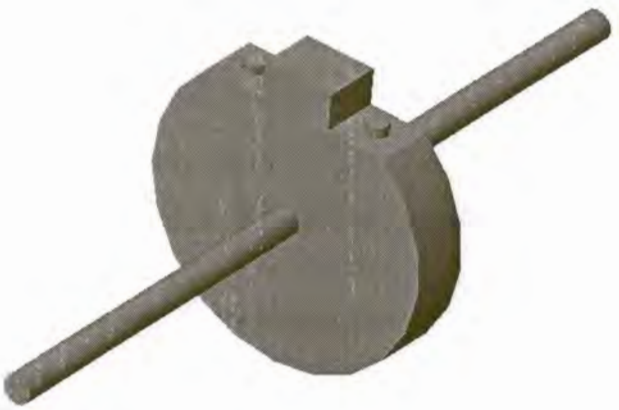

Fig. 4.8 Device used to repair "air mattresses" with discontinuities in the weld lines.

entire film to be welded. Thus, a mechanized setup is recommended for exerting the weld pressure.

(c) The use of ribbons with low coefficient of thermal expansion at the welding temperature of the adopted film is vital to obtain good, strong and uniform weld lines.

The fabricated "air mattresses" from PP and HDPE films are strong enough to be used successfully as heat transfer elements.

4.6 References

1. Hadwaco brochure, *A Quantum Leap toward Effluent-Free Industrial Plants*.

2. T. B. Scheffler, *A cost-effective multi-effect desalinator*, proceedings of IDA conference, Paradise Island, Bahamas, 2003.

3. O. Schwarz , W. Ebeling and G. Lüpke, *Plastics processing,* Translated from German

by O. C. Vorster and W. P. J. Rabé, for the Plastics Industry Training Board (PITB) South Africa, 1996.

4. O. Schwarz, *Polymer Material Handbook*, Translated from German by F-W Ebeling, H. Schirber, H. Huberth and N. Schlör, for the Plastics Industry Training Board (PITB), South Africa, 1995.

5. A.F. Mills, *Heat and Mass Transfer*, Irwin, Chicago, 1995.

6. Materials Handbook, *Properties and selection: nonferrous alloy and special purpose materials*, Volume 2, 10th edition, ASM, USA, 1990.

7. C. Maier and T. Calafut, *Polypropylene: The definitive user's guide and databook*, PDL, New York, 1998.

8. Goodfellow Catalogue, 2000